

# Relativistic transport theory of $N$ , $\Delta$ and $N^*(1440)$ interacting through $\sigma$ , $\omega$ and $\pi$ mesons \*

Guangjun Mao, L. Neise, H. Stöcker, and W. Greiner

*Institut für Theoretische Physik, J. W. Goethe-Universität  
D-60054 Frankfurt am Main, Germany*

Zhuxia Li

*Institute of Atomic Energy, P. O. Box 275(18), Beijing 102413, P. R. China*

## Abstract

A self-consistent relativistic integral-differential equation of the Boltzmann-Uehling-Uhlenbeck-type for the  $N^*(1440)$  resonance is developed based on an effective Lagrangian of baryons interacting through mesons. The closed time-path Green's function technique and semi-classical, quasi-particle and Born approximations are employed in the derivation. The non-equilibrium RBUU-type equation for the  $N^*(1440)$  is consistent with that of nucleon's and delta's which we derived before. Thus, we obtain a set of coupled equations for the  $N$ ,  $\Delta$  and  $N^*(1440)$  distribution functions. All the  $N^*(1440)$ -relevant in-medium two-body scattering cross sections within the  $N$ ,  $\Delta$  and  $N^*(1440)$  system are derived from the same effective Lagrangian in addition to the mean field and presented analytically, which can be directly used in the study of relativistic heavy-ion collisions. The theoretical

---

\*Supported by DFG-Graduiertenkolleg Theoretische & Experimentelle Schwerionenphysik, GSI, BMBF, DFG, and A.v.Humboldt-Stiftung

prediction of the free  $pp \rightarrow pp^*(1440)$  cross section is in good agreement with the experimental data. We calculate the in-medium  $N+N \rightarrow N+N^*$ ,  $N^*+N \rightarrow N+N$  and  $N^*+N \rightarrow N^*+N$  cross sections in cold nuclear matter up to twice the nuclear matter density. The influence of different choices of the  $N^*N^*$  coupling strengths, which can not be obtained through fitting certain experimental data, are discussed. The results show that the density dependence of predicted in-medium cross sections are sensitive to the  $N^*N^*$  coupling strengths used. An evident density dependence will appear when a large scalar coupling strength of  $g_{N^*N^*}^\sigma$  is assumed.

**PACS** number(s): 24.10.Cn; 25.70.-z; 21.65.+f

## I. INTRODUCTION

One of the central aims of relativistic heavy-ion collisions is to study the nuclear equation of state (EOS) under extreme conditions of high temperature and density [1, 2]. It was recognized twenty years ago that particles emitted in the collisions contain important information about the equation of state of hot and dense nuclear matter [3, 4]. Since most of the particles such as pion, kaon, dilepton, anti-proton, anti-kaon are mainly produced through resonances, the inclusion of resonance degrees of freedom in transport theories is essential for any realistic description of relativistic heavy-ion collisions. Actually, resonances produced in energetic heavy-ion collisions play as an energy-reservoir in the transport process and have strong influence on the particle production. The importance of baryon resonances on the dynamics of relativistic heavy-ion collisions as well as its effects on the particle production, especially at subthreshold energies, have been studied extensively and stressed frequently in the literature [5]-[11]. Recent theoretical calculations [12, 13] and experimental data [14] indicated that a gradual transition to *resonance matter* would occur in the collision zone at kinetic energy ranging from SIS ( $\sim 1$ AGeV) up to AGS ( $\sim 15$ AGeV). At an incident energy of 2 GeV/nucleon more than 30% of the nucleons are excited to resonance states [15]. At intermediate- and high-energy range the most important baryonic resonances are  $\Delta(1232)$ ,  $N^*(1440)$  and  $N^*(1535)$ . Theoretical models extended to describe relativistic heavy-ion collisions at this energy range should include these resonance degrees of freedom explicitly and treat them self-consistently. The heart of the problem is to determine quantitatively all possible binary collisions relating to resonances, such as  $N\Delta$ ,  $\Delta\Delta$ ,  $NN^*(1440)$ ,  $NN^*(1535)$  ... collisions. Unfortunately, very little is known about resonance-relevant in-medium cross sections in high-density nuclear matter since the experimental determination of them is inaccessible yet. In most of the transport models they are assumed to be equal to the free  $NN$  scattering cross sections. Since the density changes drastically in relativistic heavy-ion collisions the medium effects on the two-body scattering cross sections might be pronounced. This simple assumption on the resonance-relevant cross sections is quite doubtful and should be checked carefully.

Based on the different theoretical models some authors have studied the in-medium cross sections for  $NN \rightarrow N\Delta$ ,  $N\Delta \rightarrow NN$  and  $N\Delta \rightarrow N\Delta$  reactions [16, 17, 18]. Different model calculations give rather different results and the quantitative estimation of the medium dependence of in-medium  $\Delta$ -relevant cross sections has not been clear yet. It is, therefore, very important to include theoretical predicted in-medium cross sections in the transport model in order to see its effects on the physical quantities which is now experimental available. However, these in-medium cross sections, which are not calculated in the framework of transport theory, have the disadvantage that they are inconsistent with the other ingredients of the transport model when applied to the relativistic heavy-ion collision calculations, and then will cause further uncertainty on the theoretical predications.

On the other hand, the in-medium two-body scattering cross sections can be studied within the framework of transport theory, i.e., the Boltzmann-Uehling-Uhlenbeck (BUU) equation. The preliminary version of BUU-type transport equation was developed in semi-classical and non-relativistic fashion [19, 20, 21, 22]. It was then extended to the relativistic form (RBUU) [23, 24, 25]. The BUU/RBUU-type transport equation has been used extensively by several groups [19]-[26] to the study of heavy-ion collisions and turned out to be very successful. For increasing kinetic energy, it is highly desirable to develop a more general version of transport equation which includes the  $\Delta$  as well as the higher-mass resonances self-consistently, both in the mean field and in the collision term. With this in mind, several groups have set out to provide a derivation of such transport equations [27, 28]. In Refs. [29, 30] we have developed a self-consistent RBUU equation for the  $\Delta$  distribution function within the same framework we have used for the nucleon's [31]-[34]. In our approach, the  $\Delta$  isobars are treated in essentially the same way as nucleons. Both mean field and collision term of  $\Delta$ 's RBUU equation are derived from the same effective Lagrangian and presented analytically. The obtained in-medium cross sections with the  $\Delta$  resonance are consistent with the other ingredients of the transport model. Based on this approach we have studied the medium effects on all the  $N\Delta$  and  $\Delta\Delta$  scattering cross sections and its vice versa cross sections within the nucleon+ $\Delta$  system. Considerable

medium corrections have been found on the cross sections of certain channels, such as  $N + N \rightarrow N + \Delta$  and  $N + N \rightarrow \Delta + \Delta$  scattering. Our results exhibited that in the intermediate- and high-energy range the in-medium  $\Delta$ -relevant cross sections deviate substantially from the Cugnon's parameterization [35] for the free  $NN$  scattering cross section which is now commonly used in the transport model. It would be important to take the in-medium  $\Delta$ -relevant cross sections into account in the study of energetic relativistic heavy-ion collisions rather than replace it with a free  $NN$  scattering cross section. However, up to now, no investigation has been made for the in-medium  $N^*$ -relevant cross sections (the free  $N + N \rightarrow N + N^*(1440)$  scattering cross section has been studied by S. Huber and J. Aichelin within the one-boson-exchange model [36]). While  $N^*(1535)$  is essential for the production of  $\eta$ -mesons [9, 10],  $N^*(1440)$  was reported to enjoy at least equally importance as  $\Delta(1232)$  for the production of anti-protons at subthreshold energies [11].

It is the purpose of this paper to expand our theoretical framework to include the  $N^*(1440)$  degree of freedom. We will derive the self-consistent RBUU equation for the  $N^*(1440)$  distribution function within the framework we have done for the nucleon's and  $\Delta$ 's. Special attentions will be paid to the  $N^*(1440)$ -relevant in-medium cross sections. Through construction the collision term of  $N^*(1440)$ 's RBUU equation we will give the analytically expressions for calculating all the  $N^*(1440)$ -relevant in-medium two-body scattering cross sections within the  $N$ ,  $\Delta$  and  $N^*(1440)$  system. The presented cross sections are consistent with the other ingredients of the transport model and can be used directly in the study of relativistic heavy-ion collisions. The organization of the paper is as follows: in Sect. II we give the model Lagrangian and derive the RBUU equation for the  $N^*(1440)$  distribution function by means of the closed time-path Green's function technique. In Sect. III we will construct the collision term and present the analytical expressions for the in-medium differential cross sections of different channels. In Sect. IV we introduce the centroid  $N^*(1440)$  mass by taking into account the decay width of the  $N^*(1440)$  resonance. It is then used to calculate the in-medium  $N + N \rightarrow N + N^*$ ,  $N^* + N \rightarrow N + N$  and  $N^* + N \rightarrow N^* + N$  scattering cross sections. We present numerical

results in Sect. V. Finally, a summary and outlook are given in Sect. VI.

## II. RBUU-TYPE TRANSPORT EQUATION FOR THE $N^*(1440)$ DISTRIBUTION FUNCTION

In this section we will derive the self-consistent RBUU equation for the  $N^*(1440)$  distribution function. For consistency with the RBUU equations of a nucleon and a delta, here we still use the closed time-path Green's function technique. For a review of the technique we refer to Refs. [37, 38]. First of all, let us write down the total effective Lagrangian used in the model. In the framework of quantum hadrodynamics [39], the baryon-baryon interaction is described by the exchange of  $\sigma$ ,  $\omega$ ,  $\pi$  and  $\rho$  mesons. While it is well known that the mean field is mainly contributed from the  $\sigma$  and  $\omega$  mesons, some inelastic reaction channels relating to  $\Delta$  production (thus, requiring charge exchange) can only be described by the exchange of a  $\pi$  or  $\rho$  meson. However, it has been found that the pion exchange processes dominate the cross sections of single- $\Delta$  and double- $\Delta$  production from  $NN$  scattering at intermediate- and high-energy range which we are interested in, the contribution of the  $\rho$ -meson exchange is almost negligible [34, 40]. We think the situation should not be changed substantially while  $N^*(1440)$  is involved. Therefore, in the following derivation, we take the effective Lagrangian which considers the  $N$ ,  $\Delta$  and  $N^*(1440)$  system interacting through  $\sigma$ ,  $\omega$  and  $\pi$  mesons. The Lagrangian density can be written as

$$\mathcal{L} = \mathcal{L}_F + \mathcal{L}_I. \quad (1)$$

Here  $\mathcal{L}_F$  is the Lagrangian density for free nucleon, delta,  $N^*(1440)$  resonance and meson fields

$$\begin{aligned} \mathcal{L}_F = & \bar{\psi}[i\gamma_\mu\partial^\mu - M_N]\psi + \bar{\psi}^*[i\gamma_\mu\partial^\mu - M_{N^*}]\psi^* \\ & + \bar{\psi}_{\Delta\nu}[i\gamma_\mu\partial^\mu - M_\Delta]\psi_\Delta^\nu + \frac{1}{2}\partial_\mu\sigma\partial^\mu\sigma - U(\sigma) \\ & - \frac{1}{4}\omega_{\mu\nu}\omega^{\mu\nu} + U(\omega) + \frac{1}{2}(\partial_\mu\boldsymbol{\pi}\partial^\mu\boldsymbol{\pi} - m_\pi^2\boldsymbol{\pi}^2) \end{aligned} \quad (2)$$

and  $U(\sigma)$ ,  $U(\omega)$  are the self-interaction part of the scalar field [41] and vector field [42, 43]

$$U(\sigma) = \frac{1}{2}m_\sigma^2\sigma^2 + \frac{1}{3}b(g_{NN}^\sigma\sigma)^3 + \frac{1}{4}c(g_{NN}^\sigma\sigma)^4, \quad (3)$$

$$U(\omega) = \frac{1}{2}m_\omega^2\omega_\mu\omega^\mu\left(1 + \frac{(g_{NN}^\omega)^2\omega_\mu\omega^\mu}{Z^2}\right), \quad (4)$$

respectively.  $\mathcal{L}_I$  is the interaction Lagrangian density

$$\begin{aligned} \mathcal{L}_I &= \mathcal{L}_{NN} + \mathcal{L}_{N^*N^*} + \mathcal{L}_{\Delta\Delta} + \mathcal{L}_{NN^*} + \mathcal{L}_{\Delta N} + \mathcal{L}_{\Delta N^*} \\ &= g_{NN}^\sigma \bar{\psi}(x)\psi(x)\sigma(x) - g_{NN}^\omega \bar{\psi}(x)\gamma_\mu\psi(x)\omega^\mu(x) + g_{NN}^\pi \bar{\psi}(x)\gamma_\mu\gamma_5\boldsymbol{\tau} \cdot \psi(x)\partial^\mu\boldsymbol{\pi}(x) \\ &\quad + g_{N^*N^*}^\sigma \bar{\psi}^*(x)\psi^*(x)\sigma(x) - g_{N^*N^*}^\omega \bar{\psi}^*(x)\gamma_\mu\psi^*(x)\omega^\mu(x) + g_{N^*N^*}^\pi \bar{\psi}^*(x)\gamma_\mu\gamma_5\boldsymbol{\tau} \cdot \psi^*(x)\partial^\mu\boldsymbol{\pi}(x) \\ &\quad + g_{\Delta\Delta}^\sigma \bar{\psi}_{\Delta\nu}(x)\psi_{\Delta\nu}'(x)\sigma(x) - g_{\Delta\Delta}^\omega \bar{\psi}_{\Delta\nu}(x)\gamma_\mu\psi_{\Delta\nu}'(x)\omega^\mu(x) + g_{\Delta\Delta}^\pi \bar{\psi}_{\Delta\nu}(x)\gamma_\mu\gamma_5\mathbf{T} \cdot \psi_{\Delta\nu}'(x)\partial^\mu\boldsymbol{\pi}(x) \\ &\quad + [g_{NN^*}^\sigma \bar{\psi}^*(x)\psi(x)\sigma(x) - g_{NN^*}^\omega \bar{\psi}^*(x)\gamma_\mu\psi(x)\omega^\mu(x) + g_{NN^*}^\pi \bar{\psi}^*(x)\gamma_\mu\gamma_5\boldsymbol{\tau} \cdot \psi(x)\partial^\mu\boldsymbol{\pi}(x) \\ &\quad - g_{\Delta N^*}^\pi \bar{\psi}_{\Delta\mu}(x)\partial^\mu\boldsymbol{\pi}(x) \cdot \mathbf{S}^+\psi(x) - g_{\Delta N^*}^\pi \bar{\psi}_{\Delta\mu}(x)\partial^\mu\boldsymbol{\pi}(x) \cdot \mathbf{S}^+\psi^*(x) + H.c.] \\ &= g_{NN}^A \bar{\psi}(x)\Gamma_A^N\psi(x)\Phi_A(x) + g_{N^*N^*}^A \bar{\psi}^*(x)\Gamma_A^{N^*}\psi^*(x)\Phi_A(x) + g_{\Delta\Delta}^A \bar{\psi}_{\Delta\nu}(x)\Gamma_A^\Delta\psi_{\Delta\nu}'(x)\Phi_A(x) \\ &\quad + [g_{NN^*}^A \bar{\psi}^*(x)\Gamma_A^{N^*}\psi(x)\Phi_A(x) - g_{\Delta N^*}^\pi \bar{\psi}_{\Delta\mu}(x)\partial^\mu\boldsymbol{\pi}(x) \cdot \mathbf{S}^+\psi(x) \\ &\quad - g_{\Delta N^*}^\pi \bar{\psi}_{\Delta\mu}(x)\partial^\mu\boldsymbol{\pi}(x) \cdot \mathbf{S}^+\psi^*(x) + h.c.] \end{aligned} \quad (5)$$

where  $\psi$ ,  $\psi^*$  are the Dirac spinors of the nucleon and  $N^*(1440)$ , and  $\psi_{\Delta\mu}$  is the Rarita-Schwinger spinor of the  $\Delta$ -baryon.  $\boldsymbol{\tau}$  is the isospin operator of the nucleon and  $N^*(1440)$ ,  $\mathbf{T}$  is the isospin operator of the  $\Delta$ , and  $\mathbf{S}^+$  is the isospin transition operator between the isospin 1/2 and 3/2 fields.  $g_{NN}^\pi = f_\pi/m_\pi$ ,  $g_{\Delta N}^\pi = f^*/m_\pi$ ;  $\Gamma_A^N = \Gamma_A^{N^*} = \gamma_A\boldsymbol{\tau}_A$ ,  $\Gamma_A^\Delta = \gamma_A\mathbf{T}_A$ ,  $A=\sigma, \omega, \pi$ , the symbols and notation are defined in Table I.

Table I

In the language of the closed time-path Green's function technique the  $N^*(1440)$  Green's function in the interaction picture can be defined in the same way as for nucleon's by

$$iG_{N^*}(1, 2) = \langle T[\exp(-i \int dx H_I(x))\psi^*(1)\bar{\psi}^*(2)] \rangle. \quad (6)$$

Here  $T$  is the time ordering operator defined on a time contour. The corresponding Dyson equation for  $iG_{N^*}(1, 2)$  can be written as

$$iG_{N^*}(1, 2) = iG_{N^*}^0(1, 2) + \int dx_3 \int dx_4 G_{N^*}^0(1, 4)\Sigma_{N^*}(4, 3)iG_{N^*}(3, 2). \quad (7)$$

Here  $G_{N^*}^0(1, 2)$  is the zeroth-order Green's function of  $N^*(1440)$ , which is similar to that of the nucleon's zeroth-order Green's function [29, 31].  $G_{N^*}^0(1, 2)$  can be written as

$$iG_{N^*}^0(1, 2) = i \int \frac{d^4k}{(2\pi)^4} G_{N^*}^0(x, k) e^{-ik(x_1 - x_2)}, \quad (8)$$

$$G_{N^*}^{0\mp\mp}(x, k) = (\not{k} + M_{N^*}) \left[ \frac{\pm 1}{k^2 - M_{N^*}^2 \pm i\epsilon} + \frac{\pi i}{E(k)} \delta(k_0 - E(k)) f_{N^*}(x, k) \right], \quad (9)$$

$$G_{N^*}^{0+-}(x, k) = -\frac{\pi i}{E(k)} \delta(k_0 - E(k)) [1 - f_{N^*}(x, k)] (\not{k} + M_{N^*}), \quad (10)$$

$$G_{N^*}^{0-+}(x, k) = \frac{\pi i}{E(k)} \delta(k_0 - E(k)) f_{N^*}(x, k) (\not{k} + M_{N^*}). \quad (11)$$

$f_{N^*}(x, k)$  is the distribution function of  $N^*(1440)$ . As in most/all presently used RBUU-type transport models, also here we do not take into account the temperature degree of freedom. Furthermore, in our theoretical framework the negative-energy states are neglected.  $\Sigma_{N^*}(4, 3)$  is the  $N^*$  self-energy. The lowest-order self-energies contributing to the collision term come from the Born diagrams. Through considering the  $N^*$  self-energy up to the Born approximation and adopting the semi-classical approximation (in which the Green's functions and self-energies are assumed to be peaked around relative coordinate and smoothly changing with center-of-mass coordinate) and quasi-particle approximations (in which we dress the mass and momentum in the zeroth-order Green's functions appearing in the self-energy terms with the effective mass and momentum) the self-consistent RBUU equation for the  $N^*(1440)$  can be derived in the same way as that of the nucleons. The only difference between the nucleon and the  $N^*(1440)$  is the mass and the coupling strengths! Here the self-consistency means that we derive both the mean field and collision term of the transport equation simultaneously from the same effective Lagrangian. The RBUU equation for the  $N^*(1440)$  distribution function reads

$$\begin{aligned} & \{p_\mu [\partial_x^\mu - \partial_x^\mu \Sigma_{N^*}^\nu(x) \partial_\nu^p + \partial_x^\nu \Sigma_{N^*}^\mu(x) \partial_\nu^p] + m_{N^*}^* \partial_x^\nu \Sigma_{N^*}^S(x) \partial_\nu^p\} \frac{f_{N^*}(\mathbf{x}, \mathbf{p}, \tau)}{E_{N^*}^*(p)} \\ & = C^{N^*}(x, p). \end{aligned} \quad (12)$$

The left-hand side of Eq. (12) is the transport part and the right-hand side is the collision term. Here we have dropped the contribution of the Fock term, since it usually has only



small effects on the mean field. The above equation is derived within the framework as we have done for the nucleon's [31]-[34]

$$\begin{aligned} & \{p_\mu[\partial_x^\mu - \partial_x^\mu \Sigma^\nu(x) \partial_\nu^p + \partial_x^\nu \Sigma^\mu(x) \partial_\nu^p] + m^* \partial_x^\nu \Sigma^S(x) \partial_\nu^p\} \frac{f(\mathbf{x}, \mathbf{p}, \tau)}{E^*(p)} \\ & = C(x, p). \end{aligned} \quad (13)$$

and delta's [29, 30]

$$\begin{aligned} & \{p_\mu[\partial_x^\mu - \partial_x^\mu \Sigma_\Delta^\nu(x) \partial_\nu^p + \partial_x^\nu \Sigma_\Delta^\mu(x) \partial_\nu^p] + m_\Delta^* \partial_x^\nu \Sigma_\Delta^S(x) \partial_\nu^p\} \frac{f_\Delta(\mathbf{x}, \mathbf{p}, \tau)}{E_\Delta^*(p)} \\ & = C^\Delta(x, p). \end{aligned} \quad (14)$$

RBUU equations. Therefore, Eqs. (12), (13) and (14) stand in a consistent form and they are coupled together through the mean field and collision term(i.e., in-medium scattering cross sections of different channels). The  $\Sigma_{N^*}^S(x)$  and  $\Sigma_{N^*}^\mu(x)$ , which are the Hartree terms of the scalar and vector  $N^*(1440)$  self-energies, can be written as

$$\Sigma_{N^*}^S(x) = -\frac{g_{N^*N^*}^\sigma}{m_\sigma^2} [g_{NN}^\sigma \rho_S(N) + g_{N^*N^*}^\sigma \rho_S(N^*) + g_{\Delta\Delta}^\sigma \rho_S(\Delta)], \quad (15)$$

$$\Sigma_{N^*}^\mu(x) = \frac{g_{N^*N^*}^\omega}{m_\omega^2} [g_{NN}^\omega \rho_V^\mu(N) + g_{N^*N^*}^\omega \rho_V^\mu(N^*) + g_{\Delta\Delta}^\omega \rho_V^\mu(\Delta)]. \quad (16)$$

The effective four momentum and effective mass of the  $N^*(1440)$  are defined as

$$m_{N^*}^*(x) = M_{N^*} + \Sigma_{N^*}^S(x) \quad (17)$$

$$p^\mu(x) = P^\mu - \Sigma_{N^*}^\mu(x). \quad (18)$$

If one takes into account the self-interaction of the  $\sigma$ ,  $\omega$  fields given in Eqs. (3) and (4), the Eqs. (15) – (18) should be rewritten by means of the field equations of the  $\sigma$  and  $\omega$  mesons within the local density approximation

$$m_\sigma^2 \sigma(x) + b(g_{NN}^\sigma)^3 \sigma^2(x) + c(g_{NN}^\sigma)^4 \sigma^3(x) = g_{NN}^\sigma \rho_S(N) + g_{N^*N^*}^\sigma \rho_S(N^*) + g_{\Delta\Delta}^\sigma \rho_S(\Delta), \quad (19)$$

$$m_\omega^2 \omega^\mu(x) + \frac{(g_{NN}^\omega)^2 m_\omega^2}{Z^2} (\omega^\mu(x))^3 = g_{NN}^\omega \rho_V^\mu(N) + g_{N^*N^*}^\omega \rho_V^\mu(N^*) + g_{\Delta\Delta}^\omega \rho_V^\mu(\Delta), \quad (20)$$

and then

$$m_{N^*}^*(x) = M_{N^*} - g_{N^*N^*}^\sigma \sigma(x) \quad (21)$$

$$p^\mu(x) = P^\mu - g_{N^*N^*}^\omega \omega^\mu(x). \quad (22)$$

Here  $\rho_S(i)$  and  $\rho_V^\mu(i)$  are the scalar and vector densities of the nucleon,  $N^*(1440)$  and delta:

$$\rho_S(i) = \frac{\gamma(i)}{(2\pi)^3} \int d\mathbf{q} \frac{m_i^*}{\sqrt{\mathbf{q}^2 + m_i^{*2}}} f_i(\mathbf{x}, \mathbf{q}, \tau), \quad (23)$$

$$\rho_V^\mu(i) = \frac{\gamma(i)}{(2\pi)^3} \int d\mathbf{q} \frac{q^\mu}{\sqrt{\mathbf{q}^2 + m_i^{*2}}} f_i(\mathbf{x}, \mathbf{q}, \tau). \quad (24)$$

The abbreviations  $i=N, N^*, \Delta$ , and  $\gamma(i)=4, 4, 16$ , correspond to nucleon,  $N^*(1440)$  and delta, respectively. Eqs. (23) and (24) are calculated under the no-sea approximation, i.e., we drop the contribution of negative-energy states. The effective four-momenta and effective masses of nucleon and delta can be defined through substituting the appropriate nucleon and delta labels in Eqs. (21) and (22), respectively. The corresponding Feynman diagrams are given in Fig. 1.

Fig. 1

The collision term can be expressed according to the transition probability, which reads as

$$\begin{aligned} C^{N^*}(x, p) &= \frac{1}{2} \int \frac{d^3 p_2}{(2\pi)^3} \int \frac{d^3 p_3}{(2\pi)^3} \int \frac{d^3 p_4}{(2\pi)^3} (2\pi)^4 \delta^{(4)}(p + p_2 - p_3 - p_4) \\ &\quad \times W^{N^*}(p, p_2, p_3, p_4)(F_2 - F_1), \end{aligned} \quad (25)$$

where  $F_2, F_1$  are the Uehling-Uhlenbeck factors of the gain ( $F_2$ ) and loss ( $F_1$ ) terms, respectively:

$$F_2 = [1 - f_{N^*}(\mathbf{x}, \mathbf{p}, \tau)][1 - f_{B_2}(\mathbf{x}, \mathbf{p}_2, \tau)]f_{B_3}(\mathbf{x}, \mathbf{p}_3, \tau)f_{B_4}(\mathbf{x}, \mathbf{p}_4, \tau), \quad (26)$$

$$F_1 = f_{N^*}(\mathbf{x}, \mathbf{p}, \tau)f_{B_2}(\mathbf{x}, \mathbf{p}_2, \tau)[1 - f_{B_3}(\mathbf{x}, \mathbf{p}_3, \tau)][1 - f_{B_4}(\mathbf{x}, \mathbf{p}_4, \tau)], \quad (27)$$

$B_2, B_3, B_4$  can be  $N, \Delta$  and  $N^*(1440)$ .  $W^{N^*}(p, p_2, p_3, p_4)$  is the transition probability of different channels, which has the form

$$W^{N^*}(p, p_2, p_3, p_4) = \frac{1}{16E_{N^*}^*(p)E_{B_2}^*(p_2)E_{B_3}^*(p_3)E_{B_4}^*(p_4)} \sum_{AB} (T_D \Phi_D - T_E \Phi_E) + p_3 \longleftrightarrow p_4. \quad (28)$$

Here  $T_D, T_E$  are the isospin matrices and  $\Phi_D, \Phi_E$  are the spin matrices, respectively.  $D$  denotes the contribution of the direct diagrams and  $E$  is that of the exchange diagrams.  $A, B = \sigma, \omega, \pi$  represent the contributions of different mesons. The exchange of  $p_3$  and  $p_4$  is only for the case of identical particles in the final state. The two-body scattering reactions relevant to the  $N^*(1440)$  in the  $N, \Delta$  and  $N^*(1440)$  system are follows:

(1) Elastic reactions:

$$NN^* \longrightarrow NN^*, \quad \Delta N^* \longrightarrow \Delta N^*, \quad N^*N^* \longrightarrow N^*N^* .$$

(2) Inelastic reactions:

$$\begin{aligned} NN &\longleftrightarrow NN^*, & N\Delta &\longleftrightarrow NN^*, & \Delta\Delta &\longleftrightarrow NN^*, \\ NN^* &\longleftrightarrow \Delta N^*, & NN^* &\longleftrightarrow N^*N^*, & NN &\longleftrightarrow \Delta N^*, \\ N\Delta &\longleftrightarrow \Delta N^*, & \Delta\Delta &\longleftrightarrow \Delta N^*, & N^*N^* &\longleftrightarrow \Delta N^*, \\ NN &\longleftrightarrow N^*N^*, & N\Delta &\longleftrightarrow N^*N^*, & \Delta\Delta &\longleftrightarrow N^*N^*. \end{aligned}$$

In the next section we will derive the analytical expressions for the differential cross sections of the above reaction channels through calculating the concrete forms of transition probability from the Born term of the  $N^*(1440)$  self-energies. For the inelastic case we only calculate the  $N^*(1440)$ -incident cross sections, its vice versa cross sections can be obtained by means of the detailed balance [44]. The corresponding Feynman diagrams of the Born term of the  $N^*(1440)$  self-energies contributing to the different reaction channels are given in Appendix A.

### III. DERIVATION OF THE COLLISION TERM

Before coming to the calculation of the Born diagrams given in Appendix A, we firstly see if some of them are already at hand according to our previous works on the nucleon and delta scattering cross sections. Because  $N^*(1440)$  has the same coupling form as that of nucleon and the only difference is the mass and the coupling strengths, the differential cross section of the  $N^*\Delta \rightarrow N^*\Delta$  reaction should be analogous to that of the  $N\Delta \rightarrow N\Delta$  channel given in Ref. [29] except for replacing the effective mass of nucleon with that of the  $N^*(1440)$  and all the  $N$  labels on the coupling strengths with  $N^*$  labels. The same arguments apply to the  $N^*N^* \rightarrow N^*N^*$ ,  $N^*\Delta \rightarrow \Delta\Delta$ ,  $N^*\Delta \rightarrow N^*N^*$  and  $N^*N^* \rightarrow \Delta\Delta$

reactions. The corresponding cross sections can be obtained from the  $NN \rightarrow NN$  [33],  $N\Delta \rightarrow \Delta\Delta$  [29],  $N\Delta \rightarrow NN$  [31] and  $NN \rightarrow \Delta\Delta$  [34] scattering cross sections. However, for the  $NN$  elastic scattering cross section only the contribution of  $\sigma$  and  $\omega$  mesons are taken into account in Ref. [33]. For completeness, in Appendix C we give the differential cross section of  $NN$  elastic scattering including the contribution of pion. Using the same arguments, the differential cross section of the  $NN^* \rightarrow N^*N^*$  reaction can be obtained from that of the  $N^*N \rightarrow NN$  reaction by the exchange of  $m^* \leftrightarrow m_{N^*}^*$  and the labels  $N \leftrightarrow N^*$  on the coupling strengths, and so on for the  $N^*\Delta \rightarrow NN$  and  $N\Delta \rightarrow N^*N^*$  channels. In the calculations of the  $N\Delta \rightarrow N\Delta$  [29] and  $NN \rightarrow \Delta\Delta$  [34] cross sections we have found that the contribution of the exchange terms is negligible. The situation should not be changed substantially when the  $N^*(1440)$  is relevant. Therefore, we drop the exchange terms in the following derivation of the  $N^*\Delta \rightarrow N\Delta$  and  $N^*N \rightarrow \Delta\Delta$  differential cross sections. In the other reaction channels the exchange terms are taken into account.

Now let us turn to calculate the spin and isospin matrices in Eq. (28). Firstly, we consider the isospin factors  $T_D$  and  $T_E$ . Here we assume that the incident- $N^*(1440)$  has the specific isospin and account for the isospins of the other three particles, which is consistent with the fact that the RBUU equations describe coupled single-particle distribution functions. In Eq. (12) we have averaged over isospin, i.e.,  $N^*(0)$  and  $N^*(+)$ . Since  $N^*(1440)$  has the same isospin couplings as the nucleon, we can write down  $T_D$  and  $T_E$  directly based on our previous works. The isospin factors for the  $N^*N \rightarrow N^*N$ ,  $N^*N \rightarrow NN$  and  $N^*N^* \rightarrow NN$  reactions are given in Table II and III. For the  $N^*N \rightarrow N\Delta$ ,  $N^*N \rightarrow \Delta N^*$  and  $N^*N^* \rightarrow N\Delta$  reactions only the pion contributes to the cross sections due to the charge conservation, and we have  $T_D^\pi = T_E^\pi = 4$ . For the  $N^*N \rightarrow \Delta\Delta$  reaction we only consider the direct term and  $T_D^\pi = 8/3$ . For the  $N^*\Delta \rightarrow N\Delta$  reaction the isospin factors corresponding to Feynman diagram (j1) in Appendix A are given in Table IV. In diagram (j3) only the pion enters, we have  $T_D^\pi = 8/3$ . The concrete expressions for the spin matrices  $\Phi_D$  and  $\Phi_E$  are given in Appendix B.

Table II

Table III

Table IV

By means of the relation between the transition probability  $W^{N^*}(p, p_2, p_3, p_4)$  and the differential cross section [45], Eq. (25) can be rewritten as

$$C^{N^*}(x, p) = \frac{1}{2} \int \frac{d^3 p_2}{(2\pi)^3} v \sigma_{N^*}(s, t) (F_2 - F_1) d\Omega. \quad (29)$$

Here  $v$  is the Møller velocity,  $\sigma_{N^*}(s, t)$  is the differential cross section of different  $N^*$ -incident channels. By evaluating the Eqs. (B1)–(B24) and finally transforming it into a center of mass system we have obtained the analytical expressions for  $\sigma_{N^*}(s, t)$ . The in-medium  $N^*$ -incident elastic and inelastic scattering cross sections can be calculated through the following equations:

$$\sigma_{N^*N \rightarrow B_3B_4}^* = \frac{1}{8(1 + \delta_{B_3B_4})} \int \sigma_{N^*N \rightarrow B_3B_4}(s, t) d\Omega, \quad (30)$$

$$\sigma_{N^*\Delta \rightarrow B_3B_4}^* = \frac{1}{32(1 + \delta_{B_3B_4})} \int \sigma_{N^*\Delta \rightarrow B_3B_4}(s, t) d\Omega, \quad (31)$$

$$\sigma_{N^*N^* \rightarrow B_3B_4}^* = \frac{1}{8(1 + \delta_{B_3B_4})} \int \sigma_{N^*N^* \rightarrow B_3B_4}(s, t) d\Omega, \quad (32)$$

where  $B_3, B_4$  are  $N, \Delta$  and  $N^*(1440)$ . The explicit expressions of  $\sigma_{N^*N \rightarrow B_3B_4}(s, t)$ ,  $\sigma_{N^*\Delta \rightarrow B_3B_4}(s, t)$ , and  $\sigma_{N^*N^* \rightarrow B_3B_4}(s, t)$  are given in Appendix D.

#### IV. THE CENTROID $N^*(1440)$ MASS, COUPLING STRENGTHS AND FORM FACTORS

In quantum field theory all baryons are treated as elementary particles as we have done in the above derivation. But the delta and  $N^*(1440)$  are physically decay particles. It has been pointed out that the wide decay widths of resonances have strong influence on the resonance-relevant cross sections and should be taken into account [9, 44], which can be realized by introducing a distribution function of Breit-Wigner form in the collision term [34]. However, an exact treatment of Breit-Wigner function will cause difficulty in the derivation of in-medium cross sections when more than one resonance is relevant. Alternatively, we introduce a centroid  $N^*(1440)$  mass  $\langle M_{N^*} \rangle$  in the same way as we did

for the delta [31, 34], which can take into account the decay width of resonance effectively.

$\langle M_{N^*} \rangle$  is defined as

$$\langle M_{N^*} \rangle = \frac{\int_{M_N+m_\pi}^{\sqrt{S}-M_N} f(M_{N^*}) M_{N^*} dM_{N^*}}{\int_{M_N+m_\pi}^{\sqrt{S}-M_N} f(M_{N^*}) dM_{N^*}}, \quad (33)$$

$f(M_{N^*})$  is the Breit-Wigner function in the case of  $M_{N^*}$  not far away from  $M_0$

$$f(M_{N^*}) = \frac{1}{2\pi} \frac{\Gamma(q)}{(M_{N^*} - M_0)^2 + \frac{1}{4}\Gamma^2(q)}, \quad (34)$$

here  $M_0 = 1440$  MeV and  $\Gamma(q)$  is the momentum-dependent decay width of the  $N^*(1440)$  [46]

$$\Gamma(q) = \Gamma_0 \frac{M_0}{M_{N^*}} (q/q_0)^3 \frac{1.2}{1 + 0.2(\frac{q}{q_0})^2}, \quad (35)$$

where

$$q^2 = \frac{[M_{N^*}^2 - (M_N + m_\pi)^2][M_{N^*}^2 - (M_N - m_\pi)^2]}{4M_{N^*}^2}, \quad (36)$$

$q_0$  is related to the case of  $M_{N^*} = M_0$  and  $\Gamma_0 = 200$  MeV. The effect of the decay width of  $N^*(1440)$  is taken into account through replacing  $M_{N^*}$  in Eq. (21) with  $\langle M_{N^*} \rangle$ . The in-medium  $N^* + N \rightarrow N + N$  and  $N^* + N \rightarrow N^* + N$  cross sections can then be calculated by means of the equations

$$\sigma_{N^*N \rightarrow NN}^* = \frac{1}{16N} \int \sigma_{N^*N \rightarrow NN}(s, t) d\Omega, \quad (37)$$

$$\sigma_{N^*N \rightarrow N^*N}^* = \frac{1}{8} \int \sigma_{N^*N \rightarrow N^*N}(s, t) d\Omega, \quad (38)$$

here  $N$  is the normalization factor stemming from the decay width of the  $N^*(1440)$  [9, 34, 44]

$$N = \int_{(M_N+m_\pi)^2}^{(\sqrt{S}-M_N)^2} F(M_{N^*}^2) dM_{N^*}^2 \quad (39)$$

and  $F(M_{N^*}^2)$  is the Breit-Wigner function

$$F(M_{N^*}^2) = \frac{M_0}{\pi} \frac{\Gamma(q)}{(M_{N^*}^2 - M_0^2)^2 + M_0^2 \Gamma^2(q)}. \quad (40)$$

The in-medium  $N^*(1440)$  production cross section can be obtained from Eq. (37) through detailed balance [44]

$$\sigma_{NN \rightarrow NN^*}^* = \frac{1}{8} \int \frac{p_{NN^*}^2}{p_{NN}^2} \sigma_{N^*N \rightarrow NN}(s, t) d\Omega, \quad (41)$$

where  $p_{NN}$ ,  $p_{NN^*}$  denote the c. m. three momentum of the  $NN$  and  $NN^*$  states, respectively. Eqs. (37), (38) and (41) will be used in our numerical calculations.

Table V

Now let us specify the coupling strengths. For the coupling strength of  $g_{NN}^\pi$ , we take the most commonly used value  $f_\pi^2/4\pi = 0.08$ . The coupling strengths of  $g_{NN}^\sigma$  and  $g_{NN}^\omega$  are determined by fitting the known ground-state properties for infinite nuclear matter. Several sets of parameters with nonlinear self-interaction of scalar and vector field and the corresponding saturation properties are presented in Table V. For the coupling strengths of nucleon- $N^*(1440)$  coupling we follow the arguments of Ref. [36]. The following relation is expected to be valid

$$\frac{g_{NN^*}^\pi}{g_{NN}^\pi} = \frac{g_{NN^*}^\sigma}{g_{NN}^\sigma} = \frac{g_{NN^*}^\omega}{g_{NN}^\omega}. \quad (42)$$

$g_{NN^*}^\pi$  is determined from the width of pion decay of the  $N^*(1440)$ -resonance

$$\frac{g_{NN^*}^\pi}{g_{NN}^\pi} = 0.351. \quad (43)$$

For the  $N^*N^*$  coupling strengths, unfortunately, there is no any information directly from experiment available. The same situation takes place for the  $\Delta\Delta$  coupling strengths. Based on the quark model and mass splitting arguments several different choices for the delta coupling strengths have been discussed in Refs. [47, 48], which will cause strong influence on the nuclear equation of state in relativistic mean field calculations [48]. If the SU(6) symmetry is exact for baryons, one should use the universal coupling strengths, that is,

$$\alpha(\Delta) = \frac{g_{\Delta\Delta}^\omega}{g_{NN}^\omega} = 1, \quad \beta(\Delta) = \frac{g_{\Delta\Delta}^\sigma}{g_{NN}^\sigma} = 1, \quad (44)$$

here we have defined the dimensionless coupling strengths  $\alpha(\Delta)$  and  $\beta(\Delta)$ . However, the mass splitting of the multiplets show that the SU(6) symmetry is not exactly fulfilled. Then, one may assume that the coupling strengths have a splitting similar to the mass splitting of delta and nucleon

$$\alpha(\Delta) = \beta(\Delta) = \frac{M_\Delta}{M_N} \approx 1.3. \quad (45)$$

Another choice

$$\alpha(\Delta) = 1, \quad \beta(\Delta) \approx 1.3 \quad (46)$$

is based on the argument that the  $\omega$  meson has a real quark-antiquark structure while the structure of the hypothetical  $\sigma$  is not quite clear. It is worth to mention that recent calculations with the QCD sum rule method yield  $\alpha(\Delta) \approx 0.5$  while no prediction for  $\beta(\Delta)$  [49].

In numerical calculations, we assume that the above arguments apply to the  $N^*N^*$  coupling strengths. We mainly consider the following three cases:

$$\alpha(N^*) = \frac{g_{N^*N^*}^\omega}{g_{NN}^\omega} = 1, \quad \beta(N^*) = \frac{g_{N^*N^*}^\sigma}{g_{NN}^\sigma} = 1, \quad (47)$$

$$\alpha(N^*) = \beta(N^*) = \frac{M_{N^*}}{M_N} \approx 1.5. \quad (48)$$

and

$$\alpha(N^*) = 1, \quad \beta(N^*) \approx 1.5 \quad (49)$$

The influence of different choices of  $\alpha(\Delta)(\alpha(N^*))$  and  $\beta(\Delta)(\beta(N^*))$  on the predicted optical potential (the real part of self-energy) and in-medium cross sections (the imaginary part of self-energy) will be checked. For simplicity, an universal coupling strength of  $g_{\Delta\Delta}^\pi = g_{N^*N^*}^\pi = g_{NN}^\pi$  is always assumed.

To take account of the effects stemming from the finite size of hadrons and a part of the short range correlation, a phenomenological form factor is introduced at each vertex. For the nucleon-nucleon-meson vertex we take the commonly used form

$$F_{NNA}(t) = \frac{\Lambda_A^2}{\Lambda_A^2 - t}. \quad (50)$$

For the nucleon- $N^*(1440)$ -meson vertex we adopt the mixed version introduced in Ref. [31]

$$F_{NN^*A}(t, \langle M_{N^*} \rangle) = \frac{\Lambda_A^{*2}}{\Lambda_A^{*2} - t} \left[ \frac{\Gamma^2(\langle q \rangle)/4}{(\langle M_{N^*} \rangle - M_0)^2 + \Gamma_0^2/4} \right]^{1/4}, \quad (51)$$

here  $\Gamma_0 = 200$  MeV and  $\Gamma(\langle q \rangle)$  is obtained from Eqs. (35) and (36) with the  $M_{N^*}$  replaced by the centroid mass  $\langle M_{N^*} \rangle$ . Here we distinguish the form factor  $\Lambda_A^*$  for the nucleon- $N^*(1440)$ -meson vertex to the  $\Lambda_A$  for the nucleon-nucleon-meson vertex. S. Huber and



J. Aichelin claimed that  $\Lambda_A^*$  is about 40% of  $\Lambda_A$  [36]. We adopt this argument in the following calculations. The form factor of the  $N^*(1440)$ - $N^*(1440)$ -meson vertex is taken the same as that of corresponding nucleon-nucleon-meson vertex. The cut-off masses  $\Lambda_\sigma=1200$  MeV,  $\Lambda_\omega=808$  MeV and  $\Lambda_\pi=500$  MeV fixed in Refs. [31, 33, 34] will be used, which are obtained by fitting the experimental data of nucleon mean free path and the free  $NN$  scattering cross section. According to the above argument,  $\Lambda_\sigma^*=480$  MeV,  $\Lambda_\omega^*=323$  MeV. But we still take  $\Lambda_\pi^* = \Lambda_\pi=500$  MeV, since this value is already comparable to the  $\Lambda_\pi^*=400$  MeV used in Ref. [36].

## V. NUMERICAL RESULTS

Fig. 2

In this work, the numerical calculations are performed in symmetric nuclear matter at zero-temperature. The distribution functions in Eqs. (23) and (24) are replaced by the corresponding  $\theta$  functions. In Fig. 2 we display the real part of nucleon optical potential calculated with the parameters given in Table V. The computation are performed at  $\rho = \rho_0$  where there is no contribution from the delta and  $N^*(1440)$  as expected. The experimental data from phenomenological optical model analysis [50] is also presented. The nonlinear self-interaction of vector meson is known to be important for obtaining the proper density dependence of vector field at high density. But the real part of nucleon optical potential calculated with the fourth, fifth and sixth set of parameters in Table V exhibits an unreasonable momentum-dependence mainly due to the large  $\omega$  coupling strength  $g_{NN}^\omega$ . Because we will use the same coupling strengths to calculate both the mean field and in-medium scattering cross sections, this kind of unrealistic momentum-dependence exhibited by the very rapid increase of nucleon optical potential with the increase of energy will cause strange behavior of in-medium cross sections where  $\sigma$  and  $\omega$  coupling strengths enter evidently. Therefore, in the following calculations we will take only the nonlinear self-interaction of scalar field and mainly use the second set of parameters in Table V, which can also reproduce the results of the G-matrix theory [51] quite well [29].

Fig. 3

Fig. 4

Fig. 3 and Fig. 4 depict the momentum dependence of the real part of  $\Delta$  and  $N^*(1440)$  optical potential. Different sets of the  $\Delta$  and  $N^*(1440)$  coupling strengths are used. If the universal coupling strengths are assumed, the behavior as well as the well depths of the  $\Delta$  and  $N^*(1440)$  optical potential are quite similar to the nucleon optical potential. But the slopes of the curves are a little smaller because of the larger delta and  $N^*(1440)$  mass. If one takes  $\beta(\Delta) = 1.3$  ( $\beta(N^*) = 1.5$ ) but still remain  $\alpha(\Delta) = 1$  ( $\alpha(N^*) = 1$ ), a very attractive  $\Delta$  ( $N^*(1440)$ ) optical potential will be obtained compared to the nucleon optical potential. Some estimations for the  $\Delta$  optical potential were made in Refs. [52, 53]. The well depth of the delta-nucleus effective potential turns out to be  $-120$  MeV [52] and  $-150$  MeV [53], respectively. The calculations with  $\alpha(\Delta) = 1, \beta(\Delta) = 1.3$  approach to this estimation. However, one should keep in mind that no experiments for the  $\Delta$  and  $N^*(1440)$  potential are reported up to now. The above arguments should be viewed with some cautions. If the coupling strengths of  $\alpha(\Delta) = \beta(\Delta) = 1.3$  ( $\alpha(N^*) = \beta(N^*) = 1.5$ ) are used, the calculated  $\Delta$  ( $N^*(1440)$ ) optical potential becomes a little more attractive at lower energy and repulsive at higher energy compared to the case of universal coupling strengths. But no significant difference are found due to the cancellation effects of the scalar and vector field.

Fig. 5 display the density dependence of the nucleon, delta and  $N^*(1440)$  optical potential. The calculations are performed in the limit of zero-momentum ( $|\mathbf{k}| \rightarrow 0$ ). Thus, the optical potentials are essentially the summation of the scalar and vector potential of the respective baryons. Since the parameter set 2 in Table V is used as the nucleon coupling strengths, the contributions of the delta and  $N^*(1440)$  to the baryon density are negligible mainly due to the large effective mass  $m^*/M_N = 0.83$  [54, 55, 56]. In other words, we don't have density isomers on the nuclear equation of state with the present used parameters. The situation, however, will change substantially if another set of nucleon coupling strengths with smaller effective mass ( $m^*/M_N \sim 0.6$ ) is used [48, 54]. But smaller effective mass will usually cause larger  $\omega$  coupling strength ( $g_{NN}^\omega$ ).

The momentum dependence of the nucleon optical potential will then become very steep as indicated in Fig. 2. It should be mentioned that finite nuclei calculations prefer a smaller effective mass since it will give stronger spin-orbit force [43, 57, 58, 59].

The influence of different choices of the  $\Delta$  coupling strengths as well as the  $N^*(1440)$  coupling strengths on the predicted optical potentials is checked in Fig. 5. In the case of universal coupling strengths, the  $\Delta$  and  $N^*(1440)$  optical potential are the same as the nucleon optical potential. Larger scalar-delta ( $-N^*(1440)$ ) coupling strength will give a deeper  $\Delta$  ( $N^*(1440)$ ) effective-potential well depth. If one uses  $\alpha(\Delta) = 1$ ,  $\beta(\Delta) = 1.3$  ( $\alpha(N^*) = 1$ ,  $\beta(N^*) = 1.5$ ) as the  $\Delta$  ( $N^*(1440)$ ) coupling strengths, the  $\Delta$  ( $N^*(1440)$ ) potential becomes so attractive that it is still a large negative number at  $\rho = 3\rho_0$ . It is currently of urgent important to have some experimental information on the  $\Delta$  and  $N^*(1440)$  coupling strengths.

Fig. 5

Fig. 6

Now we turn to discuss the imaginary part of self-energy, i.e., the two-body scattering cross sections. Firstly, in Fig. 6 we compare our theoretical predications of free  $pp \rightarrow pp^*(1440)$  cross section to the available experimental data [60]. The results of the one-boson-exchange model computed by Huber and Aichelin [36] are also presented in this figure as dashed line. Our results are consistent with that of Ref. [36]. Both of them are in good agreement with the experimental data. Here we should point out that our calculations are almost parameter free. We do not fit any parameters to the predicted cross section. Only the argument of  $\Lambda_\sigma^*/\Lambda_\sigma = \Lambda_\omega^*/\Lambda_\omega = 40\%$  is taken from Ref. [36]. If  $\Lambda_\sigma^* = \Lambda_\sigma$  and  $\Lambda_\omega^* = \Lambda_\omega$  are adopted, the cross section will be three times larger than the empirical value at higher energy as indicated by the dotted line in the figure.

Fig. 7

Fig. 8

Fig. 7 displays the in-medium  $N^*(1440)$  production cross section at normal density, where dotted line represents the contribution of direct term and dashed line is that of exchanged term. The calculations are performed with the second set of parameters in

Table V as the nucleon coupling strengths and the universal coupling-strength assumption for the  $\Delta$  and  $N^*(1440)$  coupling strengths. In contrast to the in-medium  $\Delta$  production cross section [31], here the contribution of exchange term is negligible. Fig. 8 shows the contribution of direct term and exchange term to the in-medium  $N^* + N \rightarrow N^* + N$  cross section. It can be seen that at lower energy the exchange term plays an evident cancellation effect. With the energy increase, it decreases quickly and can be neglected at higher energy.

Fig. 9

Fig. 10

Fig. 9 and Fig. 10 depict the contributions of different mesons to the in-medium cross sections. The other conditions are the same as in Fig. 7. One can find that at lower energy the  $\sigma$  term is very large. The same situation takes place for the  $\omega$  term at higher energy. However, the  $\sigma + \omega$  mixed term has an opposite sign with that of individual  $\sigma$  and  $\omega$  terms. There exist large cancellation phenomena in the contributions of  $\sigma$  and  $\omega$  mesons. Consequently, pion contributes most at lower energy. At higher energy the  $\pi$  meson contributes nearly 1/4 of in-medium  $N + N \rightarrow N + N^*$  cross section and 1/3 of in-medium  $N^* + N \rightarrow N^* + N$  cross section. At very high energies ( $S=15-20 \text{ GeV}^2$ ), the main contribution of the  $N^* + N \rightarrow N^* + N$  cross section comes from the  $\omega$  term. Since only the exchange term remains, the contributions of  $\sigma + \pi$  and  $\omega + \pi$  mixed terms are very small.

Fig. 11

Fig. 12

Fig. 13

Fig. 11 displays the in-medium  $N^*(1440)$  production cross sections at different densities and energies. The different sets of the  $N^*(1440)$  coupling strengths are employed. For the nucleon coupling strengths we always use the parameter set2 in Table V. It is shown from Fig. 11 that the  $\sigma_{NN \rightarrow NN^*}^*$  increases with the increase of density. When the universal coupling strengths are used, only a mild dependence on the density is exhibited. The density dependence, however, will become evident if one uses a larger scalar- $N^*(1440)$

coupling strength. The choice of the  $\alpha(N^*)$  has no influence on the predicted cross sections. The reason is as follows: firstly, as one can see in Appendix D,  $g_{N^*N^*}^\omega$  does not enter the expressions of the  $\sigma_{NN \rightarrow NN^*}^*$  explicitly; secondly, we always calculate the in-medium total energy of two particle system (small s) from the incident two particles, i.e., two nucleons in the case of the  $\sigma_{NN \rightarrow NN^*}^*$ . The situation will change if one considers the  $\sigma_{N^*N \rightarrow NN}^*$ , where the influence of  $\alpha(N^*)$  will enter in the calculations of in-medium total energy (small s) from free total energy (capital S), and then affects the in-medium cross section.

Fig. 12 depicts the in-medium  $N^*(1440)$  absorption cross section. Other conditions are the same as in Fig. 11. The cross sections drop very rapidly when the energy exceeds the threshold. That means that the absorption process are most important at energy close to the threshold as in the case of  $\Delta$  absorption. When  $\alpha(N^*) = 1$ ,  $\beta(N^*) = 1.5$  is used as the  $N^*(1440)$  coupling strengths, the  $\sigma_{N^*N \rightarrow NN}^*$  exhibits an evident density dependence. It decreases with the increase of density. In other two cases, i.e.,  $\alpha(N^*) = \beta(N^*) = 1$  and  $\alpha(N^*) = \beta(N^*) = 1.5$ , the dependence of the  $\sigma_{N^*N \rightarrow NN}^*$  on the density becomes weaker and less explicit.

In Fig. 13 we show the in-medium  $N^*N \rightarrow N^*N$  cross section at different densities and energies. As can be found from the figure, the cross sections now become very sensitive to the  $\alpha(N^*)$  and  $\beta(N^*)$  used because  $g_{N^*N^*}^\sigma$  and  $g_{N^*N^*}^\omega$  enter the expressions of the  $\sigma_{N^*N \rightarrow N^*N}^*$  explicitly (see Appendix D). Generally speaking, the density dependence of the cross section is not very evident when  $\alpha(N^*) = \beta(N^*) = 1$  and  $\alpha(N^*) = \beta(N^*) = 1.5$  are used, mainly due to the strong cancellation effects from the  $\sigma + \omega$  mixed term (see Fig. 10). A strong density dependence appears when the set of  $\alpha(N^*) = 1$ ,  $\beta(N^*) = 1.5$  is used as the  $N^*(1440)$  coupling strengths. The in-medium cross section decreases with the increase of density at lower energy and increases at higher energy. As the energy changes, the cross section firstly decreases and then increases, especially in the case of  $\alpha(N^*)=1.5$ . It is mainly caused by the contribution of the  $\omega$  term. As can be seen from Fig. 10, the  $\omega$  term approaches a saturation with the increase of energy while all other terms (especially, the important cancellation term of the  $\sigma + \omega$  mixed term) decrease.

The Cugnon's parameterization for free  $NN$  elastic cross section, which is commonly used in the transport models for the  $N^*N$  elastic cross section, is also plotted in Fig. 13. One can find an evident difference between the in-medium  $N^* + N \rightarrow N^* + N$  cross section and the Cugnon's parameterization. It is therefore important to take the in-medium cross sections into account in the study of heavy-ion collisions.

## VI. SUMMARY AND OUTLOOK

Starting from the effective Lagrangian describing baryons interacting through mesons, using the closed time-path Green's function technique and adopting the semi-classical, quasi-particle and Born approximations we have developed a RBUU-type transport equation for the  $N^*(1440)$  distribution function. The equation is derived within the same framework which was successfully applied to the nucleon's [31, 33] and delta's [29] and thus we obtained a set of self-consistent equations for the  $N$ ,  $\Delta$  and  $N^*(1440)$  system. Three equations are coupled through the self-energy terms and collision terms and should be solved simultaneously in a numerical simulation of heavy-ion collisions. Both the mean field and collision term of the  $N^*(1440)$ 's RBUU equation are derived from the same effective Lagrangian and given explicitly, so the medium effects on the two-body scattering cross sections are addressed automatically and can be studied self-consistently. Therefore, this approach provides a promising way to reach a covariant description of the  $N^*(1440)$  in relativistic heavy-ion collisions.

Based on this approach, we have studied both the real part and the imaginary part of the  $N^*(1440)$  self-energy, i.e., the relativistic optical potential and the in-medium two-body scattering cross sections. Since there is no information about the  $N^*N^*$  coupling strengths available, several different choices for  $\alpha(N^*) = g_{N^*N^*}^\omega/g_{NN}^\omega$  and  $\beta(N^*) = g_{N^*N^*}^\sigma/g_{NN}^\sigma$  are investigated. The results turn out to be sensitive to the  $\alpha(N^*)$  and  $\beta(N^*)$  used. A very attractive  $N^*(1440)$  optical potential will be obtained if  $\alpha(N^*) = 1$  and  $\beta(N^*) = 1.5$  are used as the  $N^*N^*$  coupling strengths. In the case of  $\alpha(N^*) = \beta(N^*) = 1$  the  $N^*(1440)$  optical potential is similar to the nucleon optical potential. When  $\alpha(N^*) = \beta(N^*) = 1.5$ , the  $N^*(1440)$  optical potential is a little more

attractive than the nucleon optical potential at lower energy/density and more repulsive at higher energy/density. The same arguments for the  $N^*N^*$  coupling strengths are applied in the study of medium effects on the  $N + N \rightarrow N + N^*$ ,  $N^* + N \rightarrow N + N$  and  $N^* + N \rightarrow N^* + N$  scattering cross sections. Generally speaking, only a mild density-dependence of in-medium cross sections is found in the cases of  $\alpha(N^*) = \beta(N^*) = 1$  and  $\alpha(N^*) = \beta(N^*) = 1.5$ . The situation, however, is changed when the set of  $\alpha(N^*) = 1$ ,  $\beta(N^*) = 1.5$  is adopted. An evident density-dependence appears. Qualitatively, the  $\sigma_{NN \rightarrow NN^*}^*$  are found to increase with the increase of density while the  $\sigma_{N^*N \rightarrow NN}^*$  near the threshold energy decreases. For the  $\sigma_{N^*N \rightarrow N^*N}^*$ , the situation is a little complicated. It decreases with the increase of density at lower energy and increases at higher energy. Because we have not included the screening and anti-screening effects of the medium on the interaction in the present calculations, the above arguments should be viewed with caution. Further investigations are needed.

In this work the numerical calculations are performed in static nuclear matter with a spherical Fermi distribution in momentum space. In principle, the initial condition of relativistic heavy-ion collisions is related to the two interpenetrating nuclei. This kind of anisotropy of the momentum distributions have strong influence on the nuclear equation of state (i.e., mean field) when the collective velocity of the two interpenetrating nuclei is large [61, 62]. It will certainly affect the theoretical predictions of in-medium cross sections. A study of in-medium  $NN$  elastic scattering cross section in colliding nuclear matter has recently been carried out by Sehn et al. [63]. It is quite interesting to address the problem in the present transport theory, in which it can be investigated more naturally since the single-particle distribution functions of transport equations contain essentially the information of the initial longitudinal momentum excess. This output can be used in the study of heavy-ion collisions directly, both in RBUU models and in (Ur)QMD models [64]. Work on this aspect is in progress.

As has been pointed out before, the temperature degree of freedom is not taken into account in the present microscopic transport theory for non-equilibrium system. However, relativistic heavy-ion collisions allow the study of the dynamical process under extreme

conditions of high temperature and density. The temperature degree of freedom should be incorporated in order to study the phase transition. It is realized in macroscopic theories such as two/three fluid model, but it is still a major challenge to RBUU-type transport theories. Nevertheless, one can discuss the effects of temperature on the mean field and in-medium cross sections in static nuclear matter by means of the formula obtained in this work. A simpler way is to replace the single-particle distribution functions with the Fermi-Dirac distribution functions. Then one can study the temperature-dependent in-medium cross sections relativistically, which was never done before. An evident influence of temperature on the in-medium cross sections is to be expected, with implications due to investigations on the temperature-dependent imaginary part of optical potential [65].

It is straightforward to develop a transport equation for the  $N^*(1535)$  resonance within the current framework. Theoretically, the main difference between the  $N^*(1440)$  and the  $N^*(1535)$  is that the  $N^*(1535)$  has a negative parity. However, we do not think this will cause significant technical problems. The extension to the  $N^*(1535)$  will appear in forthcoming paper. As the colliding energy increases, it becomes important to include other  $N^*$  as well as  $\Delta$  resonances with higher resonance-masses. Most/all of in-medium cross sections relevant to these high-mass resonances are experimentally unavailable, and very little theoretical work on this aspect has been done. On the other hand, they are urgently needed in realistic transport models extended to describe ultra-relativistic heavy-ion collisions. These in-medium cross sections can be studied in the present microscopic transport theory. Work on this direction is continuing.

The proposed enhancement of strange particle production in heavy-ion collisions may be a very promising experimental signal in the search of quark-gluon plasma [66], connected with the possibility of existence of stable or meta-stable multistrange objects [67, 68] (which will have very important consequence on the equation of state of neutron stars [69]) has stimulated substantial further activity. Experimentally, the search for strange composites—strange clusters (MEMOs), strange droplets of quark matter (strangelets) is under investigation by a number of groups at the AGS and the SPS (e.g. E882, E814, E813/836, P864, NA52). Theoretical work about this topic receives



attention currently. With the effective Lagrangian proposed by Schaffer et al. [67, 70] the self-consistent RBUU approach is a promising model to be generalized to include the hyperon degree of freedom on the octet of spin 1/2- and decouplet of spin 3/2-baryons such as  $\Sigma$ ,  $\Xi$ ,  $\Lambda$  et al. [68]. Then, problems relevant to strangeness can be studied in a relativistic microscopic transport theory.

It should be pointed out that in this work all mesons ( $\sigma$ ,  $\omega$  and  $\pi$ ) are treated as virtual mesons. Strictly speaking, this picture is valid only under the assumption that the mesons remain in equilibrium during transport [71]. In a reasonable physical scenario, it should be possible to describe the creation and destruction of real as well as virtual mesons and not just one or the other. It is practical to firstly treat pions explicitly, considering that the pion is a physical observed meson, while the remaining other mesons, such as the  $\sigma$  and the  $\omega$  are still treated as virtual mesons [72]. It is important to develop transport equations for other physical mesons, such as  $K$ ,  $K^*$ ,  $\rho$ ,  $\eta$ ,  $\phi$ ,  $f_2$  ..., in the meson multiplets within the present framework.

It was argued that chiral symmetry might be restored or partial restored in the hot and dense matter, characterized by vanishing (dropping) effective nucleon and meson masses [73, 74]. Experimentally, this could be verified by measuring the dileptons produced from heavy-ion collisions [75]. Other experimental observations have also been cited as signals for the modification of hadron properties in nuclear matter, consistent with partial restoration of chiral symmetry. Unfortunately, almost none of them provides unambiguous evidence, since there are *conventional* mechanisms, which can generate similar effects. Although it has recently become one of the most exciting topics in nuclear physics to seek evidence of chiral symmetry restoration in heavy-ion collisions, the practical relativistic dynamical equations for describing production *with chiral symmetry* are not available yet. Derivations of such transport equations with chiral symmetry were carried out by several groups based on the chiral Lagrangian of the Nambu-Jano-Lasinio model [76, 77, 78, 79, 80]. These attempts, however, are still at an early stage and a complete numerical realization is not available as of yet. It might be numerically more practical to solve transport equations developed from an effective chiral Lagrangian with baryonic and

mesonic degrees of freedom [81, 82]. The Green's function techniques of non-equilibrium system used in this work can be directly applied to such chiral Lagrangians to develop a chiral transport theory, in which the requirement of chiral symmetry from QCD can be realized.

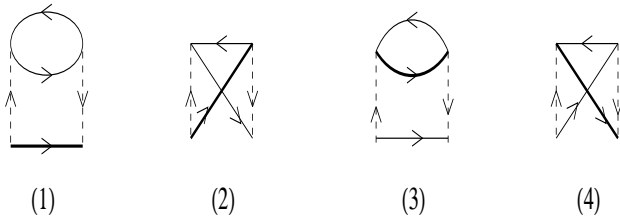
## ACKNOWLEDGMENTS

We thank S. A. Bass and C. Ernst for fruitful discussions. G. Mao and Z. Li are grateful to the Alexander von Humboldt-Stiftung for financial support and to the Institut für Theoretische Physik der J. W. Goethe Universität for their hospitality. This work was supported by DFG-Graduiertenkolleg Theoretische & Experimentelle Schwerionenphysik, GSI, BMBF, DFG, and A.v.Humboldt-Stiftung.

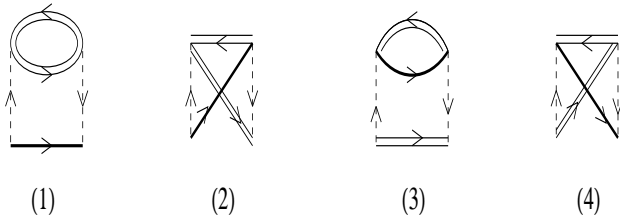
## APPENDIX A

Here we present the Feynman diagrams of the Born term of the  $N^*(1440)$  self-energies contributing to the reaction channels discussed in Sects. II and III. Dashed lines denote mesons, double lines denote deltas, and solid and bold-solid lines represent the nucleon and  $N^*(1440)$ , respectively:

(a)  $N^*N \longrightarrow N^*N$



(b)  $N^*\Delta \longrightarrow N^*\Delta$



(c)  $N^*N^* \longrightarrow N^*N^*$



(1)



(2)

(d)  $N^*N \longrightarrow NN$

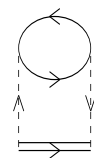


(1)



(2)

(e)  $N^*N \longrightarrow N\Delta$



(1)



(2)



(3)



(4)

(f)  $N^*N \longrightarrow \Delta\Delta$



(1)



(2)

(g)  $N^*N \longrightarrow \Delta N^*$



(1)



(2)



(3)



(4)

(h)  $N^*N \longrightarrow N^*N^*$



(1)



(2)

(i)  $N^*\Delta \longrightarrow NN$



(1)



(2)

(j)  $N^*\Delta \longrightarrow N\Delta$



(1)



(2)



(3)



(4)

(k)  $N^*\Delta \longrightarrow \Delta\Delta$



(1)



(2)

(l)  $N^*\Delta \longrightarrow N^*N^*$



(1)



(2)

(m)  $N^*N^* \longrightarrow NN$



(1)



(2)

(n)  $N^*N^* \longrightarrow N\Delta$



(1)



(2)



(3)



(4)

(o)  $N^*N^* \longrightarrow \Delta\Delta$



(1)



(2)

## APPENDIX B

In this appendix we give the concrete expressions for the spin matrices  $\Phi_D$  and  $\Phi_E$ , the subscripts denote the terms contributed from the different Feynman diagrams given in appendix A:

$$\Phi_{a1} = tr\{g_{N^*N^*}^A \gamma_A(\not{p}_3 + m_{N^*}^*) g_{N^*N^*}^B \gamma_B tr[g_{NN}^A \gamma_A(\not{p}_4 + m^*) g_{NN}^B \gamma_B(\not{p}_2 + m^*)](\not{p} + m_{N^*}^*) D_A^\mu D_B^\nu\} \frac{1}{(p-p_3)^2 - m_A^2} \frac{1}{(p-p_3)^2 - m_B^2}, \quad (B1)$$

$$\Phi_{a2} = tr\{g_{NN^*}^A \gamma_A(\not{p}_4 + m^*) g_{NN^*}^B \gamma_B(\not{p}_2 + m^*) g_{NN^*}^A \gamma_A(\not{p}_3 + m_{N^*}^*) g_{N^*N^*}^B \gamma_B(\not{p} + m_{N^*}^*) D_A^\mu D_B^\nu\} \frac{1}{(p-p_4)^2 - m_A^2} \frac{1}{(p-p_3)^2 - m_B^2}, \quad (B2)$$

$$\Phi_{a3} = tr\{g_{NN^*}^A \gamma_A(\not{p}_3 + m^*) g_{NN^*}^B \gamma_B tr[g_{NN^*}^A \gamma_A(\not{p}_4 + m_{N^*}^*) g_{NN^*}^B \gamma_B(\not{p}_2 + m^*)](\not{p} + m_{N^*}^*) D_A^\mu D_B^\nu\} \frac{1}{(p-p_3)^2 - m_A^2} \frac{1}{(p-p_3)^2 - m_B^2}, \quad (B3)$$

$$\Phi_{a4} = tr\{g_{N^*N^*}^A \gamma_A(\not{p}_4 + m_{N^*}^*) g_{NN^*}^B \gamma_B(\not{p}_2 + m^*) g_{NN}^A \gamma_A(\not{p}_3 + m^*) g_{NN^*}^B \gamma_B(\not{p} + m_{N^*}^*) D_A^\mu D_B^\nu\} \frac{1}{(p-p_4)^2 - m_A^2} \frac{1}{(p-p_3)^2 - m_B^2}, \quad (B4)$$

$$\Phi_{d1} = tr\{g_{NN^*}^A \gamma_A(\not{p}_3 + m^*) g_{NN^*}^B \gamma_B tr[g_{NN}^A \gamma_A(\not{p}_4 + m^*) g_{NN}^B \gamma_B(\not{p}_2 + m^*)](\not{p} + m_{N^*}^*) D_A^\mu D_B^\nu\} \frac{1}{(p-p_3)^2 - m_A^2} \frac{1}{(p-p_3)^2 - m_B^2}, \quad (B5)$$

$$\Phi_{d2} = tr\{g_{NN^*}^A \gamma_A(\not{p}_4 + m^*) g_{NN^*}^B \gamma_B(\not{p}_2 + m^*) g_{NN}^A \gamma_A(\not{p}_3 + m^*) g_{NN^*}^B \gamma_B(\not{p} + m_{N^*}^*) D_A^\mu D_B^\nu\} \frac{1}{(p-p_4)^2 - m_A^2} \frac{1}{(p-p_3)^2 - m_B^2}, \quad (B6)$$

$$\Phi_{e1} = -tr\{g_{\Delta N^*}^\pi (\not{p}_3 + m_\Delta^*) (p-p_3)^\nu (p-p_3)^\mu D_{\nu\mu}(p_3) g_{\Delta N^*}^\pi tr[g_{NN}^\pi (\not{p} - \not{p}_3) \gamma_5 (\not{p}_2 + m^*) g_{NN}^\pi (\not{p} - \not{p}_3) \gamma_5 (\not{p}_4 + m^*)](\not{p} + m_{N^*}^*)\} \frac{1}{(p-p_3)^2 - m_\pi^2} \frac{1}{(p-p_3)^2 - m_\pi^2}, \quad (B7)$$

$$\Phi_{e2} = -tr\{g_{NN^*}^\pi (\not{p} - \not{p}_4) \gamma_5 (\not{p}_4 + m^*) g_{NN}^\pi (\not{p} - \not{p}_3) \gamma_5 (\not{p}_2 + m^*) g_{\Delta N}^\pi (\not{p}_3 + m_\Delta^*) (p-p_4)^\rho (p-p_3)^\mu D_{\rho\mu}(p_3) g_{\Delta N^*}^\pi (\not{p} + m_{N^*}^*)\} \frac{1}{(p-p_4)^2 - m_\pi^2} \frac{1}{(p-p_3)^2 - m_\pi^2}, \quad (B8)$$

$$\Phi_{e3} = -tr\{g_{NN^*}^\pi (\not{p} - \not{p}_3) \gamma_5 (\not{p}_3 + m^*) g_{NN^*}^\pi (\not{p} - \not{p}_3) \gamma_5 tr[g_{\Delta N}^\pi (\not{p}_2 + m^*) g_{\Delta N}^\pi (\not{p}_4 + m_\Delta^*) (p-p_3)^\rho (p-p_3)^\sigma D_{\rho\sigma}(p_4)](\not{p} + m_{N^*}^*)\} \frac{1}{(p-p_3)^2 - m_\pi^2} \frac{1}{(p-p_3)^2 - m_\pi^2}, \quad (B9)$$

$$\Phi_{e4} = -tr\{g_{\Delta N^*}^\pi (\not{p}_4 + m_\Delta^*) (p-p_4)^\nu (p-p_3)^\sigma D_{\nu\sigma}(p_4) g_{\Delta N}^\pi (\not{p}_2 + m^*) g_{NN}^\pi (\not{p} - \not{p}_4) \gamma_5 (\not{p}_3 + m^*) g_{NN^*}^\pi (\not{p} - \not{p}_3) \gamma_5 (\not{p} + m_{N^*}^*)\} \frac{1}{(p-p_4)^2 - m_\pi^2} \frac{1}{(p-p_3)^2 - m_\pi^2}, \quad (B10)$$

$$\Phi_{f1} = tr\{g_{\Delta N^*}^\pi (\not{p}_3 + m_\Delta^*) (p-p_3)^\nu (p-p_3)^\mu D_{\nu\mu}(p_3) g_{\Delta N^*}^\pi tr[g_{\Delta N}^\pi (\not{p}_2 + m^*) g_{\Delta N}^\pi (\not{p}_4 + m_\Delta^*)$$

$$(p-p_3)^\rho(p-p_3)^\sigma D_{\rho\sigma}(p_4)](\not{p}+m_{N^*}^*)\left\} \frac{1}{(p-p_3)^2-m_\pi^2} \frac{1}{(p-p_3)^2-m_\pi^2}, \quad (\text{B11})$$

$$\begin{aligned} \Phi_{g1} = & -tr\{g_{\Delta N^*}^\pi(\not{p}_3+m_\Delta^*)(p-p_3)^\nu(p-p_3)^\mu D_{\nu\mu}(p_3)g_{\Delta N^*}^\pi tr[g_{N N^*}^\pi(\not{p}-\not{p}_3)\gamma_5(\not{p}_2+m^*) \\ & g_{N N^*}^\pi(\not{p}-\not{p}_3)\gamma_5(\not{p}_4+m_{N^*}^*)](\not{p}+m_{N^*}^*)\left\} \frac{1}{(p-p_3)^2-m_\pi^2} \frac{1}{(p-p_3)^2-m_\pi^2}, \quad (\text{B12}) \end{aligned}$$

$$\begin{aligned} \Phi_{g2} = & -tr\{g_{N^* N^*}^\pi(\not{p}-\not{p}_4)\gamma_5(\not{p}_4+m_{N^*}^*)g_{N N^*}^\pi(\not{p}-\not{p}_3)\gamma_5(\not{p}_2+m^*)g_{\Delta N^*}^\pi(\not{p}_3+m_\Delta^*)(p-p_4)^\rho \\ & (p-p_3)^\mu D_{\rho\mu}(p_3)g_{\Delta N^*}^\pi(\not{p}+m_{N^*}^*)\left\} \frac{1}{(p-p_4)^2-m_\pi^2} \frac{1}{(p-p_3)^2-m_\pi^2}, \quad (\text{B13}) \end{aligned}$$

$$\begin{aligned} \Phi_{g3} = & -tr\{g_{N^* N^*}^\pi(\not{p}-\not{p}_3)\gamma_5(\not{p}_3+m_{N^*}^*)g_{N^* N^*}^\pi(\not{p}-\not{p}_3)\gamma_5 tr[g_{\Delta N^*}^\pi(\not{p}_2+m^*)g_{\Delta N^*}^\pi(p_4+m_\Delta^*) \\ & (p-p_3)^\rho(p-p_3)^\sigma D_{\rho\sigma}(p_4)](\not{p}+m_{N^*}^*)\left\} \frac{1}{(p-p_3)^2-m_\pi^2} \frac{1}{(p-p_3)^2-m_\pi^2}, \quad (\text{B14}) \end{aligned}$$

$$\begin{aligned} \Phi_{g4} = & -tr\{g_{\Delta N^*}^\pi(\not{p}_4+m_\Delta^*)(p-p_4)^\nu(p-p_3)^\sigma D_{\nu\sigma}(p_4)g_{\Delta N^*}^\pi(\not{p}_2+m^*)g_{N N^*}^\pi(\not{p}-\not{p}_4) \\ & \gamma_5(\not{p}_3+m_{N^*}^*)g_{N^* N^*}^\pi(\not{p}-\not{p}_3)\gamma_5(\not{p}+m_{N^*}^*)\left\} \frac{1}{(p-p_4)^2-m_\pi^2} \frac{1}{(p-p_3)^2-m_\pi^2}, \quad (\text{B15}) \end{aligned}$$

$$\begin{aligned} \Phi_{j1} = & tr\{g_{N N^*}^A \gamma_A(\not{p}_3+m^*)g_{N N^*}^B \gamma_B tr[g_{\Delta\Delta}^B \gamma_B(\not{p}_2+m_\Delta^*)D_{\sigma\rho}(p_2)g_{\Delta\Delta}^A \gamma_A(\not{p}_4+m_\Delta^*)D^{\rho\sigma}(p_4)] \\ & (\not{p}+m_{N^*}^*)D_A^\mu D_B^\nu\left\} \frac{1}{(p-p_3)^2-m_A^2} \frac{1}{(p-p_3)^2-m_B^2}, \quad (\text{B16}) \end{aligned}$$

$$\begin{aligned} \Phi_{j3} = & tr\{g_{\Delta N^*}^\pi(\not{p}_3+m_\Delta^*)(p-p_3)^\nu(p-p_3)^\mu D_{\nu\mu}(p_3)g_{\Delta N^*}^\pi tr[g_{\Delta N^*}^\pi(\not{p}_2+m_\Delta^*)(p-p_3)^\sigma \\ & (p-p_3)^\rho D_{\sigma\rho}(p_2)g_{\Delta N^*}^\pi(\not{p}_4+m^*)](\not{p}+m_{N^*}^*)\left\} \frac{1}{(p-p_3)^2-m_\pi^2} \frac{1}{(p-p_3)^2-m_\pi^2}, \quad (\text{B17}) \end{aligned}$$

$$\begin{aligned} \Phi_{m1} = & tr\{g_{N N^*}^A \gamma_A(\not{p}_3+m^*)g_{N N^*}^B \gamma_B tr[g_{N N^*}^B \gamma_B(\not{p}_2+m_{N^*}^*)g_{N N^*}^A \gamma_A(\not{p}_4+m^*)](\not{p}+m_{N^*}^*) \\ & D_A^\mu D_B^\nu\left\} \frac{1}{(p-p_3)^2-m_A^2} \frac{1}{(p-p_3)^2-m_B^2}, \quad (\text{B18}) \end{aligned}$$

$$\begin{aligned} \Phi_{m2} = & tr\{g_{N N^*}^A \gamma_A(\not{p}_4+m^*)g_{N N^*}^B \gamma_B(\not{p}_2+m_{N^*}^*)g_{N N^*}^A \gamma_A(\not{p}_3+m^*)g_{N N^*}^B \gamma_B(\not{p}+m_{N^*}^*) \\ & D_A^\mu D_B^\nu\left\} \frac{1}{(p-p_4)^2-m_A^2} \frac{1}{(p-p_3)^2-m_B^2}, \quad (\text{B19}) \end{aligned}$$

$$\begin{aligned} \Phi_{n1} = & -tr\{g_{\Delta N^*}^\pi(\not{p}_3+m_\Delta^*)(p-p_3)^\nu(p-p_3)^\mu D_{\nu\mu}(p_3)g_{\Delta N^*}^\pi tr[g_{N N^*}^\pi(\not{p}-\not{p}_3)\gamma_5(\not{p}_2+m_{N^*}^*) \\ & g_{N N^*}^\pi(\not{p}-\not{p}_3)\gamma_5(\not{p}_4+m^*)](\not{p}+m_{N^*}^*)\left\} \frac{1}{(p-p_3)^2-m_\pi^2} \frac{1}{(p-p_3)^2-m_\pi^2}, \quad (\text{B20}) \end{aligned}$$

$$\begin{aligned} \Phi_{n2} = & -tr\{g_{N N^*}^\pi(\not{p}-\not{p}_4)\gamma_5(\not{p}_4+m^*)g_{N N^*}^\pi(\not{p}-\not{p}_3)\gamma_5(\not{p}_2+m_{N^*}^*)g_{\Delta N^*}^\pi(\not{p}_3+m_\Delta^*)(p-p_4)^\rho \\ & (p-p_3)^\mu D_{\rho\mu}(p_3)g_{\Delta N^*}^\pi(\not{p}+m_{N^*}^*)\left\} \frac{1}{(p-p_4)^2-m_\pi^2} \frac{1}{(p-p_3)^2-m_\pi^2}, \quad (\text{B21}) \end{aligned}$$

$$\begin{aligned} \Phi_{n3} = & -tr\{g_{N N^*}^\pi(\not{p}-\not{p}_3)\gamma_5(\not{p}_3+m^*)g_{N N^*}^\pi(\not{p}-\not{p}_3)\gamma_5 tr[g_{\Delta N^*}^\pi(\not{p}_2+m_{N^*}^*)g_{\Delta N^*}^\pi(\not{p}_4+m_\Delta^*) \\ & (p-p_3)^\rho(p-p_3)^\sigma D_{\rho\sigma}(p_4)](\not{p}+m_{N^*}^*)\left\} \frac{1}{(p-p_3)^2-m_\pi^2} \frac{1}{(p-p_3)^2-m_\pi^2}, \quad (\text{B22}) \end{aligned}$$

$$\begin{aligned} \Phi_{n4} = & -tr\{g_{\Delta N^*}^\pi(\not{p}_4+m_\Delta^*)(p-p_4)^\nu(p-p_3)^\sigma D_{\nu\sigma}(p_4)g_{\Delta N^*}^\pi(\not{p}_2+m_{N^*}^*)g_{N N^*}^\pi(\not{p}-\not{p}_4) \\ & \gamma_5(\not{p}_3+m^*)g_{N N^*}^\pi(\not{p}-\not{p}_3)\gamma_5(\not{p}+m_{N^*}^*)\left\} \frac{1}{(p-p_4)^2-m_\pi^2} \frac{1}{(p-p_3)^2-m_\pi^2}, \quad (\text{B23}) \end{aligned}$$

where

$$D_{\mu\nu}(p) = g_{\mu\nu} - \frac{1}{3}\gamma_\mu\gamma_\nu - \frac{1}{3m_\Delta^*}(\gamma_\mu p_\nu - \gamma_\nu p_\mu) - \frac{2}{3m_\Delta^{*2}}p_\mu p_\nu, \quad (\text{B24})$$

and  $m^*$ ,  $m_\Delta^*$  and  $m_{N^*}^*$  are the effective masses of the nucleon, delta and  $N^*(1440)$  which are defined in Sect. II.

### APPENDIX C

In this appendix we present the analytical expressions for differential cross section of in-medium  $NN$  elastic scattering including the contribution of pion. The in-medium  $N^*N^*$  elastic differential cross section can be obtained by replacing  $m^*$  with  $m_{N^*}^*$  and  $g_{NN}^A$  with  $g_{N^*N^*}^A$ .

$$\sigma_{NN \rightarrow NN}(s, t) = \frac{1}{(2\pi)^2 s} [D(s, t) + E(s, t) + (s, t \longleftrightarrow u)], \quad (\text{C1})$$

$$\begin{aligned} D(s, t) &= \frac{(g_{NN}^\sigma)^4}{2(t - m_\sigma^2)^2} (t - 4m^{*2})^2 + \frac{(g_{NN}^\omega)^4}{(t - m_\omega^2)^2} (2s^2 + 2st + t^2 - 8m^{*2}s + 8m^{*4}) \\ &+ \frac{24(g_{NN}^\pi)^4}{(t - m_\pi^2)^2} m^{*4} t^2 - \frac{4(g_{NN}^\sigma g_{NN}^\omega)^2}{(t - m_\sigma^2)(t - m_\omega^2)} (2s + t - 4m^{*2}) m^{*2}, \end{aligned} \quad (\text{C2})$$

$$\begin{aligned} E(s, t) &= -\frac{(g_{NN}^\sigma)^4}{8(t - m_\sigma^2)(u - m_\sigma^2)} [t(t + s) + 4m^{*2}(s - t)] + \frac{(g_{NN}^\omega)^4}{2(t - m_\omega^2)(u - m_\omega^2)} (s - 2m^{*2}) \\ &\times (s - 6m^{*2}) - \frac{6(g_{NN}^\pi)^4}{(t - m_\pi^2)(u - m_\pi^2)} (4m^{*2} - s - t) m^{*4} t \\ &+ (g_{NN}^\sigma g_{NN}^\omega)^2 \left[ \frac{t^2 - 4m^{*2}s - 10m^{*2}t + 24m^{*4}}{4(t - m_\sigma^2)(u - m_\omega^2)} + \frac{(t + s)^2 - 2m^{*2}s + 2m^{*2}t}{4(t - m_\omega^2)(u - m_\sigma^2)} \right] \\ &+ (g_{NN}^\sigma g_{NN}^\pi)^2 \left[ \frac{3m^{*2}(4m^{*2} - s - t)(4m^{*2} - t)}{2(t - m_\sigma^2)(u - m_\pi^2)} + \frac{3t(t + s)m^{*2}}{2(t - m_\pi^2)(u - m_\sigma^2)} \right] \\ &+ (g_{NN}^\omega g_{NN}^\pi)^2 \left[ \frac{3m^{*2}(t + s - 4m^{*2})(t + s - 2m^{*2})}{(t - m_\omega^2)(u - m_\pi^2)} + \frac{3m^{*2}(t^2 - 2m^{*2}t)}{(t - m_\pi^2)(u - m_\omega^2)} \right], \end{aligned} \quad (\text{C3})$$

where the function D represents the contribution of the direct term and E is the exchange term and

$$s = (p + p_2)^2 = [E^*(p) + E^*(p_2)]^2 - (\mathbf{p} + \mathbf{p}_2)^2, \quad (\text{C4})$$

$$t = (p - p_3)^2 = \frac{1}{2}(s - 4m^{*2})(\cos\theta - 1), \quad (\text{C5})$$

$$u = (p - p_4)^2 = 4m^{*2} - s - t, \quad (\text{C6})$$



$\theta$  is the scattering angle in c.m. system and

$$|\mathbf{p}| = |\mathbf{p}_3| = \frac{1}{2}\sqrt{s - 4m^{*2}}, \quad (\text{C7})$$

$$E^*(p) = \sqrt{\mathbf{p}^2 + m^{*2}}, \quad (\text{C8})$$

$$E^*(p_2) = \sqrt{\mathbf{p}_2^2 + m^{*2}}. \quad (\text{C9})$$

## APPENDIX D

Here we present the analytical expressions of in-medium differential cross sections for different channels.

(a) Differential cross section of in-medium  $N^*N \rightarrow N^*N$  scattering:

$$\sigma_{N^*N \rightarrow N^*N}(s, t) = \frac{1}{(2\pi)^2 s} [D(s, t) + E(s, t)], \quad (\text{D1})$$

$$\begin{aligned} D(s, t) = & \frac{(\mathbf{g}_{NN}^\sigma)^2 (\mathbf{g}_{N^*N^*}^\sigma)^2}{2(u - m_\sigma^2)^2} (4m^{*2} - u)(4m_{N^*}^{*2} - u) + \frac{(\mathbf{g}_{NN^*}^\sigma)^4}{2(t - m_\sigma^2)^2} [(m_{N^*}^{*2} + m^*)^2 - t]^2 \\ & + \frac{(\mathbf{g}_{NN}^\omega)^2 (\mathbf{g}_{N^*N^*}^\omega)^2}{(u - m_\omega^2)^2} [2(m^{*2} + m_{N^*}^{*2})^2 + s(s - 4m^{*2} - 4m_{N^*}^{*2}) + (s + u)^2] \\ & + \frac{(\mathbf{g}_{NN^*}^\omega)^4}{(t - m_\omega^2)^2} [(m_{N^*}^{*2} + m^*)^2 + (s + t)^2 + 4m^{*2}(m_{N^*}^{*2} - s) + s(s - 4m_{N^*}^{*2}) \\ & - 2(t + 2m^*m_{N^*}^*)(m_{N^*}^* - m^*)^2] + \frac{24(\mathbf{g}_{NN}^\pi)^2 (\mathbf{g}_{N^*N^*}^\pi)^2}{(u - m_\pi^2)^2} m^{*2} m_{N^*}^{*2} u^2 \\ & + \frac{3(\mathbf{g}_{NN^*}^\pi)^4}{2(t - m_\pi^2)^2} [(m_{N^*}^* - m^*)^2 - t]^2 (m_{N^*}^* + m^*)^4 \\ & + \frac{4\mathbf{g}_{NN}^\sigma \mathbf{g}_{N^*N^*}^\sigma \mathbf{g}_{NN}^\omega \mathbf{g}_{N^*N^*}^\omega}{(u - m_\sigma^2)(u - m_\omega^2)} m^* m_{N^*}^* (2m^{*2} + 2m_{N^*}^{*2} - 2s - u) \\ & + \frac{2(\mathbf{g}_{NN^*}^\sigma)^2 (\mathbf{g}_{NN^*}^\omega)^2}{(t - m_\sigma^2)(t - m_\omega^2)} [(m^{*2} + m_{N^*}^{*2})(2m^{*2} + 2m_{N^*}^{*2} - s - t) \\ & + 2m^* m_{N^*}^* (m_{N^*}^* - m^*)^2 - 2m^* m_{N^*}^* s], \quad (\text{D2}) \\ E(s, t) = & \frac{\mathbf{g}_{NN}^\sigma \mathbf{g}_{N^*N^*}^\sigma (\mathbf{g}_{NN^*}^\sigma)^2}{4(t - m_\sigma^2)(u - m_\sigma^2)} [2(m_{N^*}^{*2} - m^*)^2 + (m_{N^*}^* + m^*)^2(t - s) - st - t^2] \\ & + \frac{\mathbf{g}_{NN}^\omega \mathbf{g}_{N^*N^*}^\omega (\mathbf{g}_{NN^*}^\omega)^2}{(t - m_\omega^2)(u - m_\omega^2)} [3(m_{N^*}^{*2} + m^*)^2 - (m_{N^*}^* - m^*)^2 t \\ & + s(s - 3m^{*2} - 3m_{N^*}^{*2} - 2m^* m_{N^*}^*)] \\ & + \frac{3\mathbf{g}_{NN}^\pi \mathbf{g}_{N^*N^*}^\pi (\mathbf{g}_{NN^*}^\pi)^2}{(t - m_\pi^2)(u - m_\pi^2)} m^* m_{N^*}^* (m^* + m_{N^*}^*)^2 (2m^{*2} + 2m_{N^*}^{*2} - s - t) [(m_{N^*}^* - m^*)^2 - t] \end{aligned}$$

$$\begin{aligned}
& + \frac{(g_{NN^*}^\sigma)^2 g_{NN}^\omega g_{N^*N^*}^\omega}{2(t-m_\sigma^2)(u-m_\omega^2)} [(m_{N^*}^{*2} + m^{*2})(3(m_{N^*}^* + m^*)^2 - 3t - s) + t^2 - 2m^* m_{N^*}^* (s + 2t)] \\
& - \frac{g_{NN}^\sigma g_{N^*N^*}^\sigma (g_{NN^*}^\omega)^2}{2(u-m_\sigma^2)(t-m_\omega^2)} [4(m_{N^*}^{*2} - m^{*2})^2 + 2m^* m_{N^*}^* (s - t) - (s + t)^2] \\
& + \frac{3(g_{NN^*}^\sigma)^2 g_{NN}^\pi g_{N^*N^*}^\pi}{(t-m_\sigma^2)(u-m_\pi^2)} m^* m_{N^*}^* (2m^{*2} + 2m_{N^*}^{*2} - s - t) [(m_{N^*}^* + m^*)^2 - t] \\
& - \frac{3g_{NN}^\sigma g_{N^*N^*}^\sigma (g_{NN^*}^\pi)^2}{4(u-m_\sigma^2)(t-m_\pi^2)} (m^* + m_{N^*}^*)^2 [2(m_{N^*}^{*2} - m^{*2})^2 + (m_{N^*}^* - m^*)^2 (t - s) - st - t^2] \\
& + \frac{6(g_{NN^*}^\omega)^2 g_{NN}^\pi g_{N^*N^*}^\pi}{(t-m_\omega^2)(u-m_\pi^2)} m^* m_{N^*}^* (2m^{*2} - 2m^* m_{N^*}^* + 2m_{N^*}^{*2} - s - t) \\
& \times (2m^{*2} + 2m_{N^*}^{*2} - s - t) \\
& + \frac{3g_{NN}^\omega g_{N^*N^*}^\omega (g_{NN^*}^\pi)^2}{2(u-m_\omega^2)(t-m_\pi^2)} (m^* + m_{N^*}^*)^2 [3(m_{N^*}^{*2} + m^{*2})(m_{N^*}^* - m^*)^2 \\
& - (m_{N^*}^{*2} + m^{*2})(s + 3t) + 2m^* m_{N^*}^* (s + 2t) + t^2], \tag{D3}
\end{aligned}$$

where

$$t = \frac{1}{2}(2m_{N^*}^{*2} + 2m^{*2} - s) + \frac{1}{2s}(m_{N^*}^{*2} - m^{*2})^2 + 2|\mathbf{p}||\mathbf{p}_3|\cos\theta, \tag{D4}$$

$$u = 2m_{N^*}^{*2} + 2m^{*2} - s - t, \tag{D5}$$

$$|\mathbf{p}| = |\mathbf{p}_3| = \frac{1}{2\sqrt{s}} \sqrt{(s - m^{*2} - m_{N^*}^{*2})^2 - 4m^{*2}m_{N^*}^{*2}}. \tag{D6}$$

the definition of  $s$  is the same as in Eq. (C4),  $\theta$  is the scattering angle in c.m. system. In numerical calculations the following constraints

$$t \leq 0, \quad u \leq 0 \tag{D7}$$

must be guaranteed. Therefore

$$-1 \leq \cos\theta \leq \frac{s(s - 2m_{N^*}^{*2} - 2m^{*2}) - (m_{N^*}^{*2} - m^{*2})^2}{s(s - 2m_{N^*}^{*2} - 2m^{*2}) + (m_{N^*}^{*2} - m^{*2})^2}. \tag{D8}$$

(b) Differential cross section of in-medium  $N^*N \rightarrow NN$  scattering:

$$\sigma_{N^*N \rightarrow NN}(s, t) = \frac{1}{(2\pi)^2 s} \left[ \frac{s(s - 4m^{*2})}{(s - m^{*2} - m_{N^*}^{*2})^2 - 4m^{*2}m_{N^*}^{*2}} \right]^{1/2} [D(s, t) + E(s, t) + (s, t \longleftrightarrow u)], \tag{D9}$$

$$D(s, t) = \frac{(g_{NN}^\sigma)^2 (g_{NN^*}^\sigma)^2}{2(t - m_\sigma^2)^2} (4m^{*2} - t) [(m^* + m_{N^*}^*)^2 - t] + \frac{(g_{NN}^\omega)^2 (g_{NN^*}^\omega)^2}{(t - m_\omega^2)^2}$$

$$\begin{aligned}
& \times [2m^{*2}(m^* + m_{N^*}^*)^2 - t(m_{N^*}^* - m^*)^2 + (s+t)^2 + s(s - 6m^{*2} - 2m_{N^*}^{*2})] \\
& - \frac{6(g_{NN}^\pi)^2(g_{NN^*}^\pi)^2}{(t - m_\pi^2)^2} m^{*2} t (m^* + m_{N^*}^*)^2 [(m_{N^*}^* - m^*)^2 - t] \\
& + \frac{2g_{NN}^\sigma g_{NN^*}^\sigma g_{NN}^\omega g_{NN^*}^\omega}{(t - m_\sigma^2)(t - m_\omega^2)} m^* (m^* + m_{N^*}^*) (3m^{*2} + m_{N^*}^{*2} - 2s - t), \tag{D10}
\end{aligned}$$

$$\begin{aligned}
E(s, t) = & \frac{(g_{NN}^\sigma)^2 (g_{NN^*}^\sigma)^2}{8(t - m_\sigma^2)(u - m_\sigma^2)} [m^* (m^* + m_{N^*}^*) ((m_{N^*}^* - m^*)^2 - 2s) + t(3m^{*2} + m_{N^*}^{*2} - s - t)] \\
& + \frac{(g_{NN}^\omega)^2 (g_{NN^*}^\omega)^2}{2(t - m_\omega^2)(u - m_\omega^2)} (4m^{*2} + m^* m_{N^*}^* + m_{N^*}^{*2} - s)(m^{*2} + m^* m_{N^*}^* - s) \\
& + \frac{3(g_{NN}^\pi)^2 (g_{NN^*}^\pi)^2}{2(t - m_\pi^2)(u - m_\pi^2)} m^{*2} (m^* + m_{N^*}^*)^2 [m^* (m_{N^*}^* + m^*) (m_{N^*}^* - m^*)^2 \\
& + t(s + t - m_{N^*}^{*2} - 3m^{*2})] + \frac{g_{NN}^\sigma g_{NN^*}^\sigma g_{NN}^\omega g_{NN^*}^\omega}{4(t - m_\sigma^2)(u - m_\omega^2)} [m^* (m^* + m_{N^*}^*) \\
& \times (7m^{*2} - 2s + 4m^* m_{N^*}^* + m_{N^*}^{*2}) + t(t - 6m^{*2} - 3m^* m_{N^*}^* - m_{N^*}^{*2})] \\
& - \frac{g_{NN}^\sigma g_{NN^*}^\sigma g_{NN}^\omega g_{NN^*}^\omega}{4(u - m_\sigma^2)(t - m_\omega^2)} [2m^* (m_{N^*}^* + m^*) (m_{N^*}^* - m^*)^2 + s(2m^{*2} + m_{N^*}^{*2} - m^* m_{N^*}^*) \\
& + t(m_{N^*}^{*2} - 3m^* m_{N^*}^*) - (s + t)^2] + \frac{3g_{NN}^\sigma g_{NN^*}^\sigma g_{NN}^\pi g_{NN^*}^\pi}{4(t - m_\sigma^2)(u - m_\pi^2)} m^* (m^* + m_{N^*}^*) \\
& \times [m^{*2} (5m^{*2} + 7m^* m_{N^*}^* + 3m_{N^*}^{*2} - 2s - 5t) + m^* m_{N^*}^* (m_{N^*}^{*2} - 2s - 2t) \\
& + t(t + s - m_{N^*}^{*2})] - \frac{3g_{NN}^\sigma g_{NN^*}^\sigma g_{NN}^\pi g_{NN^*}^\pi}{4(u - m_\sigma^2)(t - m_\pi^2)} m^* (m^* + m_{N^*}^*) \\
& \times [(m_{N^*}^* - m^*)^2 (m^{*2} + m^* m_{N^*}^* + t) - st - t^2] + \frac{3g_{NN}^\omega g_{NN^*}^\omega g_{NN}^\pi g_{NN^*}^\pi}{2(t - m_\omega^2)(u - m_\pi^2)} m^* (m^* + m_{N^*}^*) \\
& \times (2m^{*2} + 2m^* m_{N^*}^* - s - t)(2m^{*2} - m^* m_{N^*}^* + m_{N^*}^{*2} - s - t) \\
& + \frac{3g_{NN}^\omega g_{NN^*}^\omega g_{NN}^\pi g_{NN^*}^\pi}{2(u - m_\omega^2)(t - m_\pi^2)} m^* (m^* + m_{N^*}^*) (m^{*2} + m^* m_{N^*}^* - t) [(m_{N^*}^* - m^*)^2 - t]. \tag{D11}
\end{aligned}$$

Here

$$t = \frac{1}{2}(3m^{*2} + m_{N^*}^{*2} - s) + 2 |\mathbf{p}| |\mathbf{p}_3| \cos \theta, \tag{D12}$$

$$u = m_{N^*}^{*2} + 3m^{*2} - s - t, \tag{D13}$$

$$|\mathbf{p}| = \frac{1}{2\sqrt{s}} \sqrt{(s - m^{*2} - m_{N^*}^{*2})^2 - 4m^{*2} m_{N^*}^{*2}}, \tag{D14}$$

$$|\mathbf{p}_3| = \frac{1}{2} \sqrt{s - 4m^{*2}}. \tag{D15}$$

(c) Differential cross section of in-medium  $N^* N \rightarrow N \Delta$  scattering:

$$\sigma_{N^* N \rightarrow N \Delta}(s, t) = \frac{1}{(2\pi)^2 s} \left[ \frac{(s - m^{*2} - m_\Delta^{*2})^2 - 4m^{*2} m_\Delta^{*2}}{(s - m^{*2} - m_{N^*}^{*2})^2 - 4m^{*2} m_{N^*}^{*2}} \right]^{1/2} [D(s, t) + E(s, t)], \tag{D16}$$

$$\begin{aligned}
D(s, t) = & -\frac{2(g_{NN}^\pi)^2(g_{\Delta N^*}^\pi)^2}{3m_{\Delta}^{*2}(u - m_\pi^2)^2} m^{*2} u [(m_{\Delta}^* + m_{N^*}^*)^2 - u]^2 [(m_{N^*}^* - m_{\Delta}^*)^2 - u] \\
& + \frac{(g_{NN^*}^\pi)^2(g_{\Delta N}^\pi)^2}{6m_{\Delta}^{*2}(t - m_\pi^2)^2} (m^* + m_{N^*}^*)^2 [(m_{\Delta}^* + m^*)^2 - t]^2 [(m_{\Delta}^* - m^*)^2 - t] \\
& [(m_{N^*}^* - m^*)^2 - t], \tag{D17}
\end{aligned}$$

$$E(s, t) = \frac{g_{NN}^\pi g_{NN^*}^\pi g_{\Delta N}^\pi g_{\Delta N^*}^\pi}{3m_{\Delta}^{*2}(t - m_\pi^2)(u - m_\pi^2)} m^* (m^* + m_{N^*}^*) \sum_{i=1}^9 E_i, \tag{D18}$$

$$\begin{aligned}
E_1 = & m_{\Delta}^{*5} m_{N^*}^* [m_{\Delta}^* m_{N^*}^* + 3m_{N^*}^{*2} - s + t] \\
& + m_{\Delta}^{*4} (m_{N^*}^{*4} - m_{N^*}^{*2} s + m_{N^*}^{*2} t - 2st + t^2), \tag{D19}
\end{aligned}$$

$$\begin{aligned}
E_2 = & m_{\Delta}^{*3} m_{N^*}^* (3m_{N^*}^{*4} - 4m_{N^*}^{*2} s - 2m_{N^*}^{*2} t + s^2 - 2st - 2t^2) \\
& + m_{\Delta}^{*2} t (2m_{N^*}^{*4} - 4m_{N^*}^{*2} s - m_{N^*}^{*2} t + 2s^2 - 2t^2), \tag{D20}
\end{aligned}$$

$$\begin{aligned}
E_3 = & m_{\Delta}^* m_{N^*}^* t [-2m_{N^*}^{*2} s - m_{N^*}^{*2} t + (2s + t)(s + t)] \\
& + m_{N^*}^{*2} t^2 (m^* t - m_{N^*}^* s - m_{N^*}^* t) + t^2 (s + t)^2, \tag{D21}
\end{aligned}$$

$$\begin{aligned}
E_4 = & m^{*2} m_{\Delta}^{*2} (2m_{\Delta}^* m_{N^*}^{*3} + 6m_{\Delta}^* m_{N^*}^* t - 2m_{N^*}^{*4} + 4m_{N^*}^{*2} s + 6m_{N^*}^{*2} t - s^2 - 2st + 7t^2) \\
& + m^{*2} m_{\Delta}^* m_{N^*}^* (2m_{N^*}^{*2} s + 4m_{N^*}^{*2} t - s^2 - 8st - 5t^2), \tag{D22}
\end{aligned}$$

$$\begin{aligned}
E_5 = & 2m^{*2} m_{N^*}^{*2} t (s + 2t) - 2m^{*2} t (s + t)(s + 3t) + m^* m_{\Delta}^{*3} (4m_{\Delta}^* m_{N^*}^{*3} - 2m_{\Delta}^* m_{N^*}^* s \\
& + 2m_{\Delta}^* m_{N^*}^* t - 4m_{N^*}^{*4} + 4m_{N^*}^{*2} s - s^2 + t^2), \tag{D23}
\end{aligned}$$

$$\begin{aligned}
E_6 = & 2m^* m_{\Delta}^* m_{N^*}^{*2} (s + t)(t - m_{\Delta}^* m_{N^*}^*) + m^* m_{\Delta}^{*2} m_{N^*}^* (s + t)(s - 3t) \\
& - m^* m_{\Delta}^* t (s + t)^2 + m^* m_{N^*}^* s t (s + 2t), \tag{D24}
\end{aligned}$$

$$\begin{aligned}
E_7 = & 2m^{*6} (2m^{*2} + 2m^* m_{\Delta}^* - 2m^* m_{N^*}^* + 2m_{\Delta}^{*2} - m_{\Delta}^* m_{N^*}^* + m_{N^*}^{*2} - 2s - 6t) \\
& + 4m^{*5} (m_{N^*}^* - m_{\Delta}^*) (s + 2t + m_{\Delta}^* m_{N^*}^*), \tag{D25}
\end{aligned}$$

$$\begin{aligned}
E_8 = & m^{*4} (-m_{\Delta}^{*4} - 3m_{\Delta}^{*3} m_{N^*}^* - 5m_{\Delta}^{*2} m_{N^*}^{*2} - 8m_{\Delta}^{*2} t - 3m_{\Delta}^* m_{N^*}^{*3} + 3m_{\Delta}^* m_{N^*}^* s \\
& + 7m_{\Delta}^* m_{N^*}^* t - m_{N^*}^{*2} s - 5m_{N^*}^{*2} t + s^2 + 10st + 13t^2), \tag{D26}
\end{aligned}$$

$$\begin{aligned}
E_9 = & m^{*3} [4m_{\Delta}^{*2} m_{N^*}^{*2} (m_{N^*}^* - m_{\Delta}^*) + 2m_{\Delta}^{*3} (s - t) + 2m_{\Delta}^* m_{N^*}^* (4m_{\Delta}^* t - m_{N^*}^* s - 3m_{N^*}^* t) \\
& + (m_{\Delta}^* - m_{N^*}^*) (s + t)(s + 5t)] + 2m^{*2} m_{\Delta}^{*4} (s - 2m_{N^*}^{*2}). \tag{D27}
\end{aligned}$$

Here

$$t = \frac{1}{2} (2m^{*2} + m_{\Delta}^{*2} + m_{N^*}^{*2} - s) + \frac{1}{2s} (m_{N^*}^{*2} - m^{*2})(m_{\Delta}^{*2} - m^{*2})$$

$$+2 |\mathbf{p}| |\mathbf{p}_3| \cos \theta, \quad (\text{D28})$$

$$u = 2m^{*2} + m_{\Delta}^{*2} + m_{N^*}^{*2} - s - t, \quad (\text{D29})$$

$$|\mathbf{p}| = \frac{1}{2\sqrt{s}} \sqrt{(s - m^{*2} - m_{N^*}^{*2})^2 - 4m^{*2}m_{N^*}^{*2}}, \quad (\text{D30})$$

$$|\mathbf{p}_3| = \frac{1}{2\sqrt{s}} \sqrt{(s - m^{*2} - m_{\Delta}^{*2})^2 - 4m^{*2}m_{\Delta}^{*2}}. \quad (\text{D31})$$

(d) Differential cross section of in-medium  $N^*N \rightarrow \Delta\Delta$  scattering:

$$\sigma_{N^*N \rightarrow \Delta\Delta}(s, t) = \frac{1}{(2\pi)^2 s} \left[ \frac{s(s - 4m_{\Delta}^{*2})}{(s - m^{*2} - m_{N^*}^{*2})^2 - 4m^{*2}m_{N^*}^{*2}} \right]^{1/2} [D(s, t) + (s, t \longleftrightarrow u)], \quad (\text{D32})$$

$$D(s, t) = \frac{(g_{\Delta N}^{\pi})^2 (g_{\Delta N^*}^{\pi})^2}{54m_{\Delta}^{*4} (t - m_{\pi}^2)^2} [(m_{\Delta}^* + m^*)^2 - t]^2 [(m_{\Delta}^* - m^*)^2 - t] \\ [(m_{N^*}^* + m_{\Delta}^*)^2 - t]^2 [(m_{N^*}^* - m_{\Delta}^*)^2 - t], \quad (\text{D33})$$

where

$$t = \frac{1}{2}(2m_{\Delta}^{*2} + m^{*2} + m_{N^*}^{*2} - s) + 2 |\mathbf{p}| |\mathbf{p}_3| \cos \theta, \quad (\text{D34})$$

$$u = 2m_{\Delta}^{*2} + m^{*2} + m_{N^*}^{*2} - s - t, \quad (\text{D35})$$

$$|\mathbf{p}| = \frac{1}{2\sqrt{s}} \sqrt{(s - m^{*2} - m_{N^*}^{*2})^2 - 4m^{*2}m_{N^*}^{*2}}, \quad (\text{D36})$$

$$|\mathbf{p}_3| = \frac{1}{2} \sqrt{s - 4m_{\Delta}^{*2}}. \quad (\text{D37})$$

(e) Differential cross section of in-medium  $N^*N \rightarrow \Delta N^*$  scattering:

$$\sigma_{N^*N \rightarrow \Delta N^*}(s, t) = \frac{1}{(2\pi)^2 s} \left[ \frac{(s - m_{\Delta}^{*2} - m_{N^*}^{*2})^2 - 4m_{\Delta}^{*2}m_{N^*}^{*2}}{(s - m^{*2} - m_{N^*}^{*2})^2 - 4m^{*2}m_{N^*}^{*2}} \right]^{1/2} [D(s, t) + E(s, t)], \quad (\text{D38})$$

$$D(s, t) = \frac{(g_{N N^*}^{\pi})^2 (g_{\Delta N^*}^{\pi})^2}{6m_{\Delta}^{*2} (u - m_{\pi}^2)^2} (m^* + m_{N^*}^*)^2 [(m_{N^*}^* - m^*)^2 - u] [(m_{N^*}^* + m_{\Delta}^*)^2 - u]^2 \\ \times [(m_{N^*}^* - m_{\Delta}^*)^2 - u] - \frac{2(g_{N^* N^*}^{\pi})^2 (g_{\Delta N}^{\pi})^2}{3m_{\Delta}^{*2} (t - m_{\pi}^2)^2} m_{N^*}^{*2} t [(m_{\Delta}^* + m^*)^2 - t]^2 \\ \times [(m_{\Delta}^* - m^*)^2 - t], \quad (\text{D39})$$

$$E(s, t) = \frac{g_{N N^*}^{\pi} g_{N^* N^*}^{\pi} g_{\Delta N}^{\pi} g_{\Delta N^*}^{\pi}}{3m_{\Delta}^{*2} (t - m_{\pi}^2) (u - m_{\pi}^2)} m_{N^*}^* (m^* + m_{N^*}^*) \sum_{i=1}^8 E_i, \quad (\text{D40})$$

$$\begin{aligned}
E_1 = & -m^{*2}t^2(4s + 3t) + m^*m_{\Delta}^{*4}m_{N^*}^*(m_{\Delta}^*m_{N^*}^* + m_{N^*}^{*2} - s + t) \\
& + m^*m_{\Delta}^{*2}t(-2m_{\Delta}^*s + m_{\Delta}^*t + 2m_{N^*}^{*3} - 2m_{N^*}^*s), \tag{D41}
\end{aligned}$$

$$\begin{aligned}
E_2 = & m^*m_{\Delta}^*t(m_{N^*}^{*4} - 2m_{N^*}^{*2}s + m_{N^*}^{*2}t + s^2 - t^2) + m^*m_{N^*}^*t^2(m_{N^*}^{*2} - s - t) \\
& + m_{\Delta}^{*5}m_{N^*}^*(m_{\Delta}^*m_{N^*}^* + m_{N^*}^{*2} - s + t), \tag{D42}
\end{aligned}$$

$$\begin{aligned}
E_3 = & m_{\Delta}^{*4}(t^2 - 2st) + m_{\Delta}^{*2}t(-2m_{\Delta}^*m_{N^*}^*t + 2m_{N^*}^{*4} - 4m_{N^*}^{*2}s + m_{N^*}^{*2}t + 2s^2 - 2t^2) \\
& + m_{\Delta}^*m_{N^*}^*t^2(-m_{N^*}^{*2} + s + t), \tag{D43}
\end{aligned}$$

$$E_4 = m_{N^*}^{*2}t^2(m_{N^*}^{*2} - 2s - 2t) + t^2(s + t)^2, \tag{D44}$$

$$\begin{aligned}
E_5 = & m^{*5}(m^{*2}m_{N^*}^* + m^*m_{\Delta}^*m_{N^*}^* - m^*t - 2m_{\Delta}^{*2}m_{N^*}^* + m_{\Delta}^*m_{N^*}^{*2} \\
& - m_{\Delta}^*t + m_{N^*}^{*3} - m_{N^*}^*s - 3m_{N^*}^*t), \tag{D45}
\end{aligned}$$

$$\begin{aligned}
E_6 = & m^{*4}(-2m_{\Delta}^{*3}m_{N^*}^* + m_{\Delta}^{*2}m_{N^*}^{*2} + m_{\Delta}^*m_{N^*}^{*3} - m_{\Delta}^*m_{N^*}^*s - m_{\Delta}^*m_{N^*}^*t \\
& - 2m_{N^*}^{*2}t + 2st + 3t^2), \tag{D46}
\end{aligned}$$

$$\begin{aligned}
E_7 = & m^{*3}(m_{\Delta}^{*4}m_{N^*}^* - 2m_{\Delta}^{*3}m_{N^*}^{*2} + 2m_{\Delta}^{*3}t - 2m_{\Delta}^{*2}m_{N^*}^{*3} + 2m_{\Delta}^{*2}m_{N^*}^*s + 2m_{\Delta}^{*2}m_{N^*}^*t \\
& - 2m_{\Delta}^*m_{N^*}^{*2}t + 2m_{\Delta}^*t^2 - 2m_{N^*}^{*3}t + 2m_{N^*}^*st + 3m_{N^*}^*t^2), \tag{D47}
\end{aligned}$$

$$\begin{aligned}
E_8 = & m^{*2}(m_{\Delta}^{*5}m_{N^*}^* - 2m_{\Delta}^{*4}m_{N^*}^{*2} + 2m_{\Delta}^{*4}t - 2m_{\Delta}^{*3}m_{N^*}^{*3} + 2m_{\Delta}^{*3}m_{N^*}^*s - 2m_{\Delta}^{*2}st \\
& + 2m_{\Delta}^{*2}t^2 - m_{\Delta}^*m_{N^*}^*t^2 - m_{N^*}^{*4}t + 2m_{N^*}^{*2}st + 4m_{N^*}^{*2}t^2 - s^2t]. \tag{D48}
\end{aligned}$$

Here

$$\begin{aligned}
t = & \frac{1}{2}(2m_{N^*}^{*2} + m^{*2} + m_{\Delta}^{*2} - s) - \frac{1}{2s}(m_{N^*}^{*2} - m^{*2})(m_{N^*}^{*2} - m_{\Delta}^{*2}) \\
& + 2|\mathbf{p}||\mathbf{p}_3|\cos\theta, \tag{D49}
\end{aligned}$$

$$u = 2m_{N^*}^{*2} + m^{*2} + m_{\Delta}^{*2} - s - t, \tag{D50}$$

$$|\mathbf{p}| = \frac{1}{2\sqrt{s}}\sqrt{(s - m^{*2} - m_{N^*}^{*2})^2 - 4m^{*2}m_{N^*}^{*2}}, \tag{D51}$$

$$|\mathbf{p}_3| = \frac{1}{2\sqrt{s}}\sqrt{(s - m_{\Delta}^{*2} - m_{N^*}^{*2})^2 - 4m_{\Delta}^{*2}m_{N^*}^{*2}}. \tag{D52}$$

(f) Differential cross section of in-medium  $N^*\Delta \rightarrow N\Delta$  scattering:

$$\sigma_{N^*\Delta \rightarrow N\Delta}(s, t) = \frac{1}{(2\pi)^2s} \left[ \frac{(s - m^{*2} - m_{\Delta}^{*2})^2 - 4m^{*2}m_{\Delta}^{*2}}{(s - m_{\Delta}^{*2} - m_{N^*}^{*2})^2 - 4m_{\Delta}^{*2}m_{N^*}^{*2}} \right]^{1/2} [D(s, t) + E(s, t)], \tag{D53}$$

$$D(s, t) = \frac{(g_{NN^*}^{\sigma})^2(g_{\Delta\Delta}^{\sigma})^2}{9m_{\Delta}^{*4}(u - m_{\sigma}^2)^2} (4m_{\Delta}^{*2} - u)(18m_{\Delta}^{*4} - 6m_{\Delta}^{*2}u + u^2)[(m_{N^*}^* + m^*)^2 - u]$$

$$\begin{aligned}
& -\frac{2(g_{NN^*}^\omega)^2(g_{\Delta\Delta}^\omega)^2}{9m_\Delta^{*4}(u-m_\omega^2)^2} \{(2m_\Delta^{*2}-u)^2[(m_{N^*}^*-m^*)^2u-2(m^*m_{N^*}^*+m_\Delta^{*2})^2] \\
& +2s(2m_\Delta^{*2}+m_{N^*}^{*2}+m^{*2}-s-u)-u^2\} + 2m^{*2}m_\Delta^{*4}(14s+5u-2m^{*2}-10m_{N^*}^{*2}) \\
& -4m^*m_\Delta^{*4}m_{N^*}^*(14m_\Delta^{*2}+u)+2m_\Delta^{*4}(28m_\Delta^{*2}s-14m_\Delta^{*4}-2m_{N^*}^{*4}+14m_{N^*}^{*2}s+5m_{N^*}^{*2}u \\
& -14s^2-14su-3u^2)\} + \frac{4g_{NN^*}^\sigma g_{NN^*}^\omega g_{\Delta\Delta}^\sigma g_{\Delta\Delta}^\omega}{9m_\Delta^{*3}(u-m_\sigma^2)(u-m_\omega^2)}(m^{*2}+2m_\Delta^{*2}+m_{N^*}^{*2}-2s-u) \\
& \times(m^*+m_{N^*}^*)(18m_\Delta^{*4}-6m_\Delta^{*2}u+u^2)-\frac{5(g_{NN^*}^\pi)^2(g_{\Delta\Delta}^\pi)^2}{3m_\Delta^{*2}(u-m_\pi^2)^2}u(m^*+m_{N^*}^*)^2 \\
& \times(10m_\Delta^{*4}-2m_\Delta^{*2}u+u^2)[(m_{N^*}^*-m^*)^2-u]+\frac{(g_{\Delta N^*}^\pi)^2(g_{\Delta N^*}^\pi)^2}{54m_\Delta^{*4}(t-m_\pi^2)^2}[(m_\Delta^*+m^*)^2-t]^2 \\
& \times[(m_\Delta^*-m^*)^2-t][(m_{N^*}^*+m_\Delta^*)^2-t]^2[(m_{N^*}^*-m_\Delta^*)^2-t], \tag{D54}
\end{aligned}$$

Here

$$\begin{aligned}
t &= \frac{1}{2}(2m_\Delta^{*2}+m^{*2}+m_{N^*}^{*2}-s)-\frac{1}{2s}(m_{N^*}^{*2}-m_\Delta^{*2})(m_\Delta^{*2}-m^{*2}) \\
& +2|\mathbf{p}||\mathbf{p}_3|\cos\theta, \tag{D55}
\end{aligned}$$

$$u = 2m_\Delta^{*2}+m^{*2}+m_{N^*}^{*2}-s-t, \tag{D56}$$

$$|\mathbf{p}| = \frac{1}{2\sqrt{s}}\sqrt{(s-m_\Delta^{*2}-m_{N^*}^{*2})^2-4m_\Delta^{*2}m_{N^*}^{*2}}, \tag{D57}$$

$$|\mathbf{p}_3| = \frac{1}{2\sqrt{s}}\sqrt{(s-m^{*2}-m_\Delta^{*2})^2-4m^{*2}m_\Delta^{*2}}. \tag{D58}$$

(g) Differential cross section of in-medium  $N^*N^* \rightarrow NN$  scattering:

$$\sigma_{N^*N^* \rightarrow NN}(s,t) = \frac{1}{(2\pi)^2s} \left[ \frac{s-4m^{*2}}{s-4m_{N^*}^{*2}} \right]^{1/2} [D(s,t) + E(s,t) + (s,t \longleftrightarrow u)], \tag{D59}$$

$$\begin{aligned}
D(s,t) &= \frac{(g_{NN^*}^\sigma)^4}{2(t-m_\sigma^2)^2}[(m_{N^*}^*+m^*)^2-t]^2 + \frac{(g_{NN^*}^\omega)^4}{(t-m_\omega^2)^2}[(m^{*2}+m_{N^*}^{*2})^2 \\
& -2(m_{N^*}^*-m^*)^2(t+2m^*m_{N^*}^*)+2s(s+t-2m^{*2}-2m_{N^*}^{*2})+4m^{*2}m_{N^*}^{*2}+t^2] \\
& + \frac{3(g_{NN^*}^\pi)^4}{2(t-m_\pi^2)^2}(m^*+m_{N^*}^*)^4[(m_{N^*}^*-m^*)^2-t]^2 \\
& + \frac{2(g_{NN^*}^\sigma)^2(g_{NN^*}^\omega)^2}{(t-m_\sigma^2)(t-m_\omega^2)}[(m_{N^*}^*+m^*)^2(2m^*m_{N^*}^*-s)-2m^*m_{N^*}^*t], \tag{D60}
\end{aligned}$$

$$\begin{aligned}
E(s,t) &= -\frac{(g_{NN^*}^\sigma)^4}{8(t-m_\sigma^2)(u-m_\sigma^2)}[(m_{N^*}^{*2}-m^{*2})^2+(m_{N^*}^*+m^*)^2s+t(s+t-2m^{*2}-2m_{N^*}^{*2})] \\
& + \frac{(g_{NN^*}^\omega)^4}{2(t-m_\omega^2)(u-m_\omega^2)}(12m^{*2}m_{N^*}^{*2}-3m^{*2}s-2m^*m_{N^*}^*s-3m_{N^*}^{*2}s+s^2)
\end{aligned}$$

$$\begin{aligned}
& + \frac{3(g_{NN^*}^\pi)^4}{8(t - m_\pi^2)(u - m_\pi^2)}(m^* + m_{N^*}^*)^4[(m_{N^*}^{*2} - m^{*2})^2 + (m_{N^*}^* - m^*)^2 s \\
& + t(s + t - 2m^{*2} - 2m_{N^*}^{*2})] + \frac{(g_{NN^*}^\sigma)^2(g_{NN^*}^\omega)^2}{4(t - m_\sigma^2)(u - m_\omega^2)}[(m_{N^*}^{*2} - m^{*2})^2 + (m_{N^*}^* + m^*)^2 \\
& \times (6m^*m_{N^*}^* - s - 2t) + t(t - 2m^*m_{N^*}^*)] + \frac{(g_{NN^*}^\sigma)^2(g_{NN^*}^\omega)^2}{4(u - m_\sigma^2)(t - m_\omega^2)}[(m_{N^*}^{*2} - m^{*2})^2 \\
& - (m_{N^*}^* - m^*)^2(6m^*m_{N^*}^* + 3s + 2t) + 2m^*m_{N^*}^*(t - s) + (s + t)^2] \\
& + \frac{3(g_{NN^*}^\sigma)^2(g_{NN^*}^\pi)^2}{8(t - m_\sigma^2)(u - m_\pi^2)}(m^* + m_{N^*}^*)^2[(m_{N^*}^* + m^*)^2 - s - t][(m_{N^*}^* + m^*)^2 - t] \\
& + \frac{3(g_{NN^*}^\sigma)^2(g_{NN^*}^\pi)^2}{8(u - m_\sigma^2)(t - m_\pi^2)}(m^* + m_{N^*}^*)^2[(m_{N^*}^* - m^*)^2 - s - t][(m_{N^*}^* - m^*)^2 - t] \\
& + \frac{3(g_{NN^*}^\omega)^2(g_{NN^*}^\pi)^2}{4(t - m_\omega^2)(u - m_\pi^2)}(m^* + m_{N^*}^*)^2[(m_{N^*}^{*2} + m^{*2})^2 - (m_{N^*}^* + m^*)^2(s + 2t) \\
& + 2m^*m_{N^*}^*(m^{*2} + m_{N^*}^{*2} - s + t) + (s + t)^2] + \frac{3(g_{NN^*}^\omega)^2(g_{NN^*}^\pi)^2}{4(u - m_\omega^2)(t - m_\pi^2)}(m^* + m_{N^*}^*)^2 \\
& \times [(m_{N^*}^{*2} + m^{*2})^2 + (m_{N^*}^* - m^*)^2(s - 2t) - 2m^*m_{N^*}^*(m^{*2} + m_{N^*}^{*2} + t) + t^2], \quad (D61)
\end{aligned}$$

where

$$t = \frac{1}{2}(2m^{*2} + 2m_{N^*}^{*2} - s) + 2 |\mathbf{p}| |\mathbf{p}_3| \cos \theta, \quad (D62)$$

$$u = 2m^{*2} + 2m_{N^*}^{*2} - s - t, \quad (D63)$$

$$|\mathbf{p}| = \frac{1}{2}\sqrt{s - 4m_{N^*}^{*2}}, \quad (D64)$$

$$|\mathbf{p}_3| = \frac{1}{2}\sqrt{s - 4m^{*2}}. \quad (D65)$$

(h) Differential cross section of in-medium  $N^*N^* \rightarrow N\Delta$  scattering:

$$\sigma_{N^*N^* \rightarrow N\Delta}(s, t) = \frac{1}{(2\pi)^2 s} \left[ \frac{(s - m^{*2} - m_\Delta^{*2})^2 - 4m^{*2}m_\Delta^{*2}}{s(s - 4m_{N^*}^{*2})} \right]^{1/2} [D(s, t) + E(s, t) + (s, t \longleftrightarrow u)], \quad (D66)$$

$$\begin{aligned}
D(s, t) &= \frac{(g_{NN^*}^\pi)^2(g_{\Delta N^*}^\pi)^2}{6m_\Delta^{*2}(t - m_\pi^2)^2}(m^* + m_{N^*}^*)^2[(m_{N^*}^* - m^*)^2 - t] \\
& \quad [(m_{N^*}^* + m_\Delta^*)^2 - t]^2[(m_{N^*}^* - m_\Delta^*)^2 - t], \quad (D67)
\end{aligned}$$

$$E(s, t) = \frac{(g_{NN^*}^\pi)^2(g_{\Delta N^*}^\pi)^2}{12m_\Delta^{*2}(t - m_\pi^2)(u - m_\pi^2)}(m^* + m_{N^*}^*)^2 \sum_{i=1}^{10} E_i, \quad (D68)$$

$$E_1 = m_\Delta^{*2}(6m_{N^*}^{*4}t + m_{N^*}^{*2}s^2 - 8m_{N^*}^{*2}st + 2s^2t - 2t^3)$$



$$+m_{\Delta}^* m_{N^*}^* (3m_{N^*}^{*4} s - m_{N^*}^{*2} s^2 - 6m_{N^*}^{*2} st + 3s^2 t + 3st^2), \quad (\text{D69})$$

$$E_2 = m_{N^*}^{*2} (m_{N^*}^{*6} - 4m_{N^*}^{*4} t - m_{N^*}^{*2} s^2 + 2m_{N^*}^{*2} st + 6m_{N^*}^{*2} t^2 - 4st^2 - 4t^3) \\ + t^2 (s + t)^2, \quad (\text{D70})$$

$$E_3 = 2m_{N^*}^{*2} t^2 (2m_{N^*}^{*2} - s - t) + m_{\Delta}^* m_{N^*}^{*4} (-m_{\Delta}^* m_{N^*}^* + 3m_{N^*}^{*2} - s + t) \\ + m_{\Delta}^* m_{N^*}^{*3} (4m_{N^*}^{*2} - s + 2t), \quad (\text{D71})$$

$$E_4 = m_{\Delta}^* m_{N^*}^{*2} m_{N^*}^{*3} (-m_{N^*}^{*2} + 4s + 2t) - m_{\Delta}^* m_{N^*}^{*2} m_{N^*}^* (s^2 + t^2) \\ + m_{\Delta}^* m_{N^*}^* (-2m_{N^*}^{*4} s + m_{N^*}^{*2} s^2 + 4m_{N^*}^{*2} st - 2s^2 t - 2st^2), \quad (\text{D72})$$

$$E_5 = m_{\Delta}^* m_{N^*}^* (-m_{N^*}^{*4} s + m_{N^*}^{*2} s^2 + 2m_{N^*}^{*2} st - s^2 t - st^2) \\ + m_{\Delta}^{*5} m_{N^*}^* (m_{\Delta}^* m_{N^*}^* + 5m_{N^*}^{*2} - s + t), \quad (\text{D73})$$

$$E_6 = m_{\Delta}^{*4} (3m_{N^*}^{*4} - 2m_{N^*}^{*2} s + 4m_{N^*}^{*2} t - 2st + t^2) + m_{\Delta}^{*2} m_{N^*}^* (-m_{\Delta}^* m_{N^*}^{*4} - 4m_{\Delta}^* m_{N^*}^{*2} s \\ + 2m_{\Delta}^* m_{N^*}^{*2} t + m_{\Delta}^* s^2 - 4m_{\Delta}^* st - m_{\Delta}^* t^2 - 4m_{N^*}^{*5}), \quad (\text{D74})$$

$$E_7 = m_{\Delta}^{*5} m_{N^*}^* (m_{\Delta}^{*2} - m_{\Delta}^* m_{N^*}^* + m_{N^*}^{*2} - t) + m_{\Delta}^{*4} (m_{\Delta}^{*4} + m_{\Delta}^{*3} m_{N^*}^* \\ + m_{\Delta}^{*2} m_{N^*}^{*2} - 2m_{\Delta}^{*2} t + 3m_{\Delta}^* m_{N^*}^{*3} - m_{\Delta}^* m_{N^*}^* t - m_{N^*}^{*4} + t^2), \quad (\text{D75})$$

$$E_8 = m_{\Delta}^{*3} (-m_{\Delta}^{*4} m_{N^*}^* + 2m_{\Delta}^{*3} m_{N^*}^{*2} - 2m_{\Delta}^{*3} s - 4m_{\Delta}^{*2} m_{N^*}^{*3} + 2m_{\Delta}^* st \\ + m_{N^*}^{*5} - 2m_{N^*}^{*3} s - 2m_{N^*}^{*3} t + 2m_{N^*}^* st + m_{N^*}^* t^2), \quad (\text{D76})$$

$$E_9 = m_{\Delta}^{*2} m_{\Delta}^{*4} (-m_{\Delta}^* m_{N^*}^* - 6m_{N^*}^{*2} + 2s - 2t) + m_{\Delta}^{*2} m_{\Delta}^{*3} (-8m_{N^*}^{*3} + 4m_{N^*}^* s) \\ + 2m_{\Delta}^{*2} m_{\Delta}^{*2} (2m_{N^*}^{*4} - m_{N^*}^{*2} s + 2t^2), \quad (\text{D77})$$

$$E_{10} = m_{\Delta}^{*2} m_{N^*}^* (m_{\Delta}^* m_{N^*}^{*4} - 2m_{\Delta}^* m_{N^*}^{*2} s - 2m_{\Delta}^* m_{N^*}^{*2} t - 2m_{\Delta}^* st + m_{\Delta}^* t^2 \\ + 2m_{N^*}^{*3} s - 2m_{N^*}^{*3} t), \quad (\text{D78})$$

where

$$t = \frac{1}{2} (2m_{N^*}^{*2} + m^{*2} + m_{\Delta}^{*2} - s) + 2 |\mathbf{p}| |\mathbf{p}_3| \cos \theta, \quad (\text{D79})$$

$$u = 2m_{N^*}^{*2} + m^{*2} + m_{\Delta}^{*2} - s - t, \quad (\text{D80})$$

$$|\mathbf{p}| = \frac{1}{2} \sqrt{s - 4m_{N^*}^{*2}}, \quad (\text{D81})$$

$$|\mathbf{p}_3| = \frac{1}{2\sqrt{s}} \sqrt{(s - m^{*2} - m_{\Delta}^{*2})^2 - 4m^{*2} m_{\Delta}^{*2}} \quad (\text{D82})$$

## References

- [1] H. G. Baumgardt, J. U. Schott, Y. Sakamoto, E. Schopper, H. Stöcker, J. Hofmann, W. Scheid and W. Greiner, *Z. Phys.* **A273**, 359 (1975).
- [2] J. Hofmann, H. Stöcker, U. Heinz, W. Scheid, and W. Greiner, *Phys. Rev. Lett.* **36**, 88 (1976).
- [3] G. F. Chapline, M. H. Johnson, E. Teller, and M. S. Weiss, *Phys. Rev.* **D8**, 4302 (1973).
- [4] H. Stöcker, W. Greiner, W. Scheid, *Z. Phys.* **A286**, 121 (1978).
- [5] M. Hofmann, R. Mattiello, N. S. Amelin, M. Berenguer, A. Dumitru, A. Jahns, A. v. Keitz, Y. Pürsün, T. Schönfeld, C. Spieles, L. A. Winckelmann, H. Sorge, J. A. Maruhn, H. Stöcker and W. Greiner, *Nucl. Phys.* **A566**, 15c (1994).
- [6] J. Aichelin and C. M. Ko, *Phys. Rev. Lett.* **55**, 2661 (1985).
- [7] G. Q. Li, C. M. Ko, and X. S. Fang, *Phys. Lett.* **B329**, 149 (1994).
- [8] G. Q. Li, C. M. Ko, X. S. Fang, and Y. M. Zheng, *Phys. Rev.* **C49**, 1139 (1994).
- [9] Gy. Wolf, W. Cassing, and U. Mosel, *Nucl. Phys.* **A545**, 139c (1992); *Nucl. Phys.* **A552**, 549 (1993).
- [10] F.-D. Berg, M. Pfeiffer, O. Schwalb et al., *Phys. Rev. Lett.* **72**, 977 (1994).
- [11] Bao-An Li, C. M. Ko and G. Q. Li, *Phys. Rev.* **C50**, R2675 (1994).
- [12] W. Ehehalt, W. Cassing, A. Engel, U. Mosel and Gy. Wolf, *Phys. Rev.* **C47**, R2467 (1993).
- [13] M. Hofmann, R. Mattiello, H. Sorge, H. Stöcker and W. Greiner, *Phys. Rev.* **C51**, 2095 (1995).
- [14] V. Metag, *Nucl. Phys.* **A553**, 283c (1993).

- [15] R. Auerbeck, R. Holzmann, A. Schubert et al., GSI Sci. Rep., 80 (1994).
- [16] B. ter Haar and R. Malfliet, Phys. Rev. **C36**, 1611 (1987).
- [17] G. F. Bertsch, G. E. Brown, V. Koch, and B. A. Li, Nucl. Phys. **A490**, 745 (1988).
- [18] T.-S. H. Lee, Phys. Rev. **C54**, 1350 (1996).
- [19] J. J. Molitoris, J. B. Hoffer, H. Kruse and H. Stöcker, Phys. Rev. Lett. **53**, 899 (1984).
- [20] H. Kruse, B. V. Jacak and H. Stöcker, Phys. Rev. Lett. **54**, 289 (1985).
- [21] H. Stöcker and W. Greiner, Phys. Rep. **137**, 277 (1986).
- [22] G. F. Bertsch and S. Das Gupta, Phys. Rep. **160**, 189 (1988)
- [23] H.-Th. Elze, M. Gyulassy, D. Vasak, H. Heinz, H. Stöcker, and W. Greiner, Mod. Phys. Lett. **2**, 451 (1987).
- [24] C. M. Ko, Q. Li, and R. Wang, Phys. Rev. Lett. **59**, 1084 (1987); Q. Li, J. Q. Wu, and C. M. Ko, Phys. Rev. **C39**, 849 (1989).
- [25] B. Blättel, V. Koch, W. Cassing, and U. Mosel, Phys. Rev. **C38**, 1767 (1988).
- [26] W. Cassing, V. Metag, U. Mosel and K. Niita, Phys. Rep. **188**, 363 (1990).
- [27] Shun-Jin Wang, Bao-An Li, Wolfgang Bauer, and Jørgen Randrup, Ann. Phys. **209**, 251 (1991).
- [28] M. Schönhofen, M. Cubero, M. Gering, M. Sambataro, H. Feldmeier, and W. Nörenberg, Nucl. Phys. **A504**, 875 (1989); M. Schönhofen, M. Cubero, B. L. Friman, W. Nörenberg, and Gy. Wolf, Nucl. Phys. **A572**, 112 (1994).
- [29] Guangjun Mao, Zhuxia Li, Yizhong Zhuo, Phys. Rev. **C53**, 2933 (1996).
- [30] Guangjun Mao, Zhuxia Li, Yizhong Zhuo, and Enguang Zhao, Phys. Lett. **B378**, 5 (1996).

- [31] Guangjun Mao, Zhuxia Li, Yizhong Zhuo, Yinlu Han, and Ziqiang Yu, Phys. Rev. **C49**, 3137 (1994); Guangjun Mao, Zhuxia Li, Yizhong Zhuo, and Ziqiang Yu, Phys. Lett. **B327**, 183 (1994).
- [32] Zhuxia Li, Guangjun Mao, Yizhong Zhuo, in *Proceedings of the NATO ASI on Hot and Dense Nuclear Matter*, Bodrum, Turkey, **Vol. 335**, 659 (Plenum, New York, 1994).
- [33] Mao Guangjun, Li Zhuxia, Zhuo Yizhong, Han Yinlu, Yu Ziqiang and M. Sano, Z. Phys. **A347**, 173 (1994).
- [34] Guangjun Mao, Zhuxia Li, Yizhong Zhuo, and Enguang Zhao, Phys. Rev. **C55**, 792 (1997).
- [35] J. Cugnon, T. Mizutani and J. Vandermeulen, Nucl. Phys. **A352**, 505 (1981).
- [36] S. Huber and J. Aichelin, Nucl. Phys. **A573**, 587 (1994)
- [37] P. Danielewicz, Ann. Phys. (N.Y.) **152**, 239 (1984).
- [38] Kuangchao Chou, Zhaobin Su, Bailin Hao, and Lu Yu, Phys. Rep. **118**, 1 (1985).
- [39] B. D. Serot and J. D. Walecka, Adv. Nucl. Phys. **16**, 1 (1986).
- [40] A. Engel, R. Shyam, U. Mosel, and A.K. Dutt-Mazumder, Nucl. Phys. **A603**, 387 (1996).
- [41] J. Boguta and H. Stöcker, Phys, Lett. **B120**, 289 (1983).
- [42] A. R. Bodmer, Nucl. Phys. **A526**, 703 (1991).
- [43] Y. Sugahara, H. Toki, Nucl. Phys. **A579**, 557 (1994).
- [44] P. Danielewicz and G. F. Bertsch, Nucl. Phys. **A533**, 712 (1991).
- [45] S. R. de Groot, W. A. van Leeuwen, and Ch. G. van Weert, *Relativistic Kinetic Theory* (North-Holland, Amsterdam, 1980).

- [46] S. A. Bass, PhD thesis, Frankfurt university, unpublished.
- [47] S.A. Moszkowski, Phys. Rev. **D9**, 1613 (1974); S.I.A. Garpman, N.K. Glendenning and Y.J. Karant, Nucl. Phys. **A322**, 382 (1979).
- [48] B.M. Waldhauser, J. Theis, J.A. Maruhn, H. Stöcker and W. Greiner, Phys. Rev. **C36**, 1019 (1987); P. Lévai, B. Lukács, B. Waldhauser and J. Zimányi, Phys. Lett. **B177**, 5 (1986).
- [49] Xuemin Jin, Phys. Rev. **C51**, 2260 (1995).
- [50] S. Hama, B. C. Clark, E. D. Cooper, H. S. Sherif, and R. L. Mercer, Phys. Rev. **C41**, 2737 (1990)
- [51] R. Brockmann and R. Machleidt, Phys. Rev. **C42**, 1965 (1990)
- [52] J. Boguta, Phys. Lett. **B109**, 251 (1982); J. Boguta and H. Stöcker, Phys. Lett. **B120**, 289 (1983).
- [53] M. Danos and H.T. Williams, Phys. Lett. **B89**, 169 (1980).
- [54] Zhuxia Li, Guangjun Mao, Yizhong Zhuo and W. Greiner, Phys. Rev. **C56**, 1570 (1997).
- [55] Guangjun Mao, Zhuxia Li, and Yizhong Zhuo, Commun. Theor. Phys. **26**, 223 (1996).
- [56] Tetsuo Nakai and Shuji Takagi, Prog. Theor. Phys. **71**, 1118 (1984).
- [57] P.-G. Reinhard, M. Rufa, J. Maruhn, W. Greiner, J. Friedrich, Z. Phys. **A323**, 13 (1986).
- [58] M. Rufa, P.-G. Reinhard, J.A. Maruhn, W. Greiner, M.R. Strayer, Phys. Rev. **C38**, 390 (1988).
- [59] Y.K. Gambhir, P. Ring, and A. Thimet, Ann. Phys. **198**, 132 (1990).

- [60] CERN-HERA Report 83-01.
- [61] I. Lovas, Nucl. Phys. **A367**, 509 (1981).
- [62] L. Neise, H. Stöcker and W. Greiner, J. Phys. G: Nucl. Phys. **13**, L181 (1987).
- [63] L. Sehn, H.H. Wolter, Nucl. Phys. **A601**, 473 (1996); C. Fuchs, L. Sehn, H.H. Wolter, Nucl. Phys. **A601**, 505 (1996).
- [64] S. A. Bass, UrQMD collaboration, H. Stöcker and W. Greiner, to be published.
- [65] Han Yinlu, Zhang Zhengjun, and Sun Xiuquan, Phys. Rev. **C55**, 2838 (1997).
- [66] P. Koch, B. Müller and J. Rafelski, Phys. Rep. **142**, 167 (1986); C. Greiner, D.H. Rischke, H. Stöcker, P. Koch, Phys. Rev. **D38**, 2797 (1988).
- [67] J. Schaffner, C.B. Dover, A. Gal, C. Greiner and H. Stöcker, Phys. Rev. Lett. **71**, 1328 (1993).
- [68] W. Greiner, Int. J. Mod. Phys. **E5**, 1 (1996).
- [69] N.K. Glendenning, F. Weber, S.A. Moszkowski, Phys. Rev. **C45**, 844 (1992).
- [70] J. Schaffner, C.B. Dover, A. Gal, C. Greiner and H. Stöcker, *Proceeding of The NATO ASI on Hot and Dense Nuclear Matter*, Bodrum, Turkey; Vol. 335, 255(Plenum, New York, 1994);
- [71] John E. Davis and Robert J. Perry, Phys. Rev. **C43**, 1893 (1991).
- [72] Guangjun Mao, L. Neise, H. Stöcker, and W. Greiner, in preparation.
- [73] G.E. Brown and Mannque Rho, Phys. Rev. Lett. **66**, 2720 (1991).
- [74] M.C. Birse, J. Phys. **G20:Nucl. Phys.**, 1537 (1994).
- [75] G.Q. Li, C.M. Ko, and G.E. Brown, Phys. Rev. Lett. **75**, 4007 (1995).
- [76] Wei-Min Zhang and Lawrence Willets, Phys. Rev. **C45**, 1900 (1992).

- [77] A. Abada and J. Aichelin, Phys. Rev. Lett. **74**, 3130 (1995).
- [78] C. Greiner and D. Rischke, Phys. Rev. **C54**, 1360 (1996).
- [79] L.P. Csernai and I.N. Mishustin, Phys. Rev. Lett. **74**, 5005 (1995).
- [80] S.P. Klevansky, A. Ogura and J. Hüfner, hep-ph/9708263.
- [81] P. Papazoglou, J. Schaffner, S. Schramm, D. Zschesche, H. Stöcker, and W. Greiner, Phys. Rev. **C55**, 1499 (1997).
- [82] P. Papazoglou, S. Schramm, J. Schaffner-Bielich, H. Stöcker, W. Greiner, submitted to Phys. Rev. C.

## TABLES

**TABLE I:** Some symbols and notation used in this paper,  $k_\mu$  is the transformed four-momentum.

A	$m_A$	$g_{NN}^A$	$g_{N^*N^*}^A$	$g_{\Delta\Delta}^A$	$g_{NN^*}^A$	$\gamma_A$	$\tau_A$	$T_A$	$\Phi_A(x)$	$D_A^\mu$	$D_A^i$
$\sigma$	$m_\sigma$	$g_{NN}^\sigma$	$g_{N^*N^*}^\sigma$	$g_{\Delta\Delta}^\sigma$	$g_{NN^*}^\sigma$	1	1	1	$\sigma(x)$	1	1
$\omega$	$m_\omega$	$-g_{NN}^\omega$	$-g_{N^*N^*}^\omega$	$-g_{\Delta\Delta}^\omega$	$-g_{NN^*}^\omega$	$\gamma_\mu$	1	1	$\omega^\mu(x)$	$-g^{\mu\nu}$	1
$\pi$	$m_\pi$	$g_{NN}^\pi$	$g_{N^*N^*}^\pi$	$g_{\Delta\Delta}^\pi$	$g_{NN^*}^\pi$	$\not{k}\gamma_5$	$\boldsymbol{\tau}$	$\mathbf{T}$	$\boldsymbol{\pi}(x)$	1	$\delta_{ij}$

**TABLE II:** Isospin factors for the direct term of  $N^*N \rightarrow N^*N$ ,  $N^*N \rightarrow NN$  and  $N^*N^* \rightarrow NN$  reactions.

$\Gamma_D^{AB}$	$\sigma$	$\omega$	$\pi$
$\sigma$	2	2	0
$\omega$	2	2	0
$\pi$	0	0	6

**TABLE III:** Isospin factors for the exchange term of  $N^*N \rightarrow N^*N$ ,  $N^*N \rightarrow NN$  and  $N^*N^* \rightarrow NN$  reactions.

$\Gamma_E^{AB}$	$\sigma$	$\omega$	$\pi$
$\sigma$	1	1	3
$\omega$	1	1	3
$\pi$	3	3	-3



**TABLE IV:** Isospin factors for the direct term of  $N^*\Delta \rightarrow N\Delta$  reaction (corresponding to Feynman diagram (j1) in Appendix A).

$T_D^{AB}$	$\sigma$	$\omega$	$\pi$
$\sigma$	4	4	0
$\omega$	4	4	0
$\pi$	0	0	15

**TABLE V:** Mean field parameters and the corresponding nuclear saturation properties. The sixth set is the TM1 parameters from Ref. [43].

	$g_{NN}^\sigma$	$g_{NN}^\omega$	$b(g_{NN}^\sigma)^3$	$c(g_{NN}^\sigma)^4$	Z	$E_{\text{bin}}$	$m^*/M_N$	K(MeV)	$\rho_0$
1	9.40	10.95	-0.69	40.44	$\infty$	-15.57	0.70	380	0.145
2	6.90	7.54	-40.49	383.07	$\infty$	-15.76	0.83	380	0.145
3	7.937	6.696	42.35	157.55	$\infty$	-16.00	0.85	210	0.153
4	12.419	15.063	12.276	189.008	1.7042	-15.29	0.60	210	0.185
5	11.536	14.528	-4.252	102.141	2.8335	-15.56	0.60	310	0.150
6	10.029	12.614	-7.233	0.6183	5.9273	-16.30	0.634	281	0.145

## CAPTIONS

**Fig.1** Feynman diagrams contributing to the Hartree term of the (a) nucleon, (b) delta and (c)  $N^*(1440)$  self-energies. A dashed line denotes a meson, a double line denotes the delta resonance, a solid and bold-solid line represent the nucleon and the  $N^*(1440)$ , respectively.

**Fig.2** The relativistic nucleon optical potential calculated at  $\rho = \rho_0$  as a function of the kinetic energy. The different curves correspond to the different parameter sets (Table V) as indicated in the figure. The hatched area shows the experimental data from Ref. [50].

**Fig.3** The momentum dependence of the relativistic  $\Delta$  optical potential calculated at  $\rho = \rho_0$ . The second set of parameters in Table V is used as the nucleon coupling strengths. For the delta coupling strengths several different choices are tested and discussed in the text.

**Fig.4** The same as Fig. 3, but for the  $N^*(1440)$  optical potential.

**Fig.5** The density dependence of the nucleon, delta and  $N^*(1440)$  optical potential calculated in the limit of zero-momentum. The parameter set2 in Table V is used as the nucleon coupling strengths. The different choices of the delta and  $N^*(1440)$  coupling strengths are employed in the calculations and discussed in the text.

**Fig.6** Free scattering cross section for reaction  $pp \rightarrow pp^*(1440)$ . The parameter set2 in Table V is used as the nucleon coupling strengths. Solid line represents the results of this work, and dashed line denotes the results of Ref. [36]. The experimental data are taken from Ref. [60]. The unitary form factor for  $NN$  and  $NN^*$  vertex, i.e.,  $\Lambda_A^* = \Lambda_A$  is also tested in the calculations, which is depicted by the dotted line.

**Fig.7** The in-medium  $NN \rightarrow NN^*$  cross section at normal density. The parameter set2 in Table V is used as the nucleon coupling strengths. For the  $\Delta$  and  $N^*(1440)$

coupling strengths we employ the universal coupling-strength assumption. The contributions of the direct term and exchange term are denoted by the dotted and dashed line, respectively. The solid line gives the summation of these two terms.

Fig.8 The same as Fig. 7, but for an in-medium  $N^*N \rightarrow N^*N$  cross section.

Fig.9 The contributions of different terms to the in-medium  $NN \rightarrow NN^*$  cross section. Others are the same as in Fig. 7.

Fig.10 The same as Fig. 9, but for an in-medium  $N^*N \rightarrow N^*N$  cross section.

Fig.11 The in-medium  $NN \rightarrow NN^*$  cross section at different densities and energies. The calculations are performed with parameter set2 in Table V and different sets of  $\alpha(N^*)$  and  $\beta(N^*)$ .

Fig.12 The same as Fig. 11, but for an in-medium  $N^*N \rightarrow NN$  cross section.

Fig.13 The same as Fig. 11, but for an in-medium  $N^*N \rightarrow N^*N$  cross section.

Fig. 1

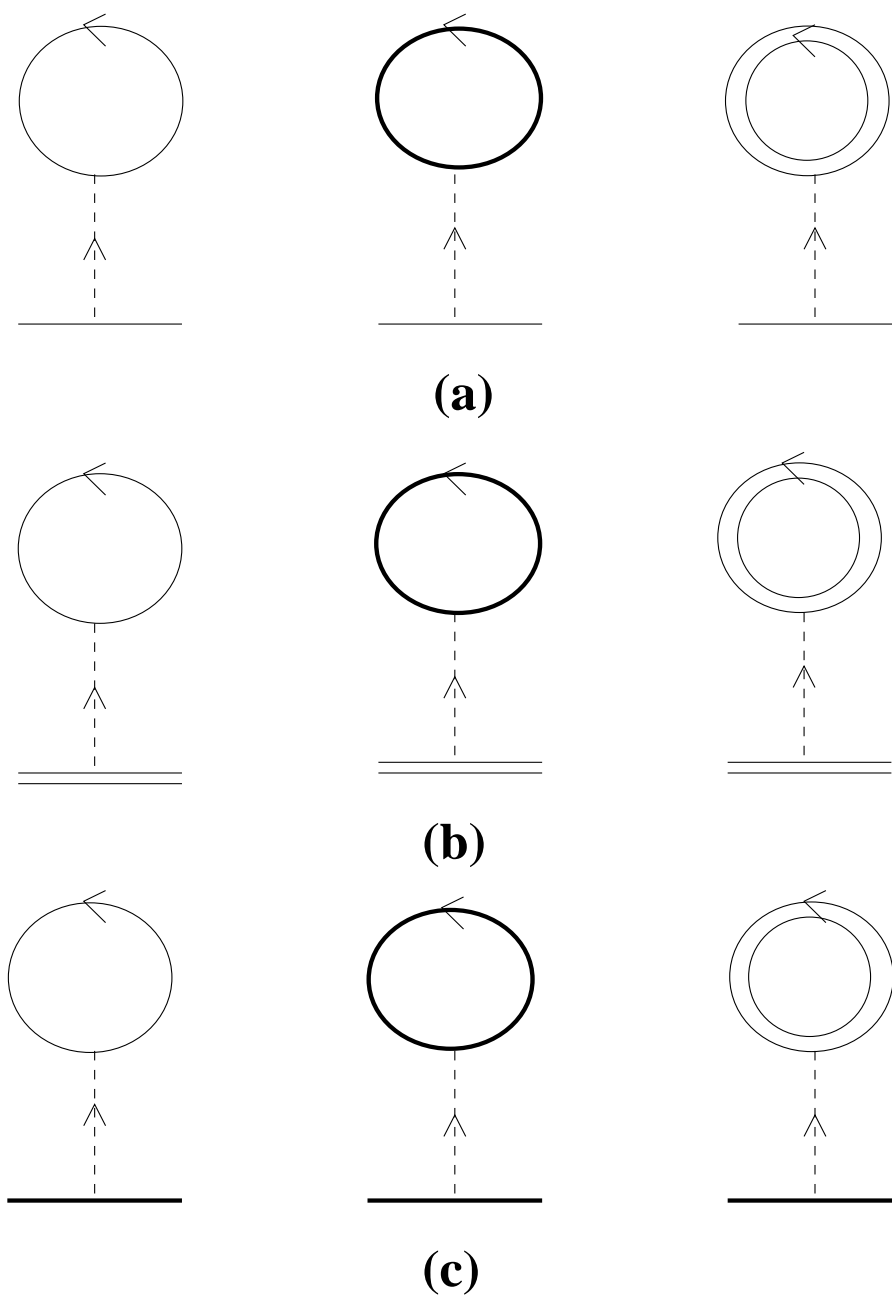


Fig. 2

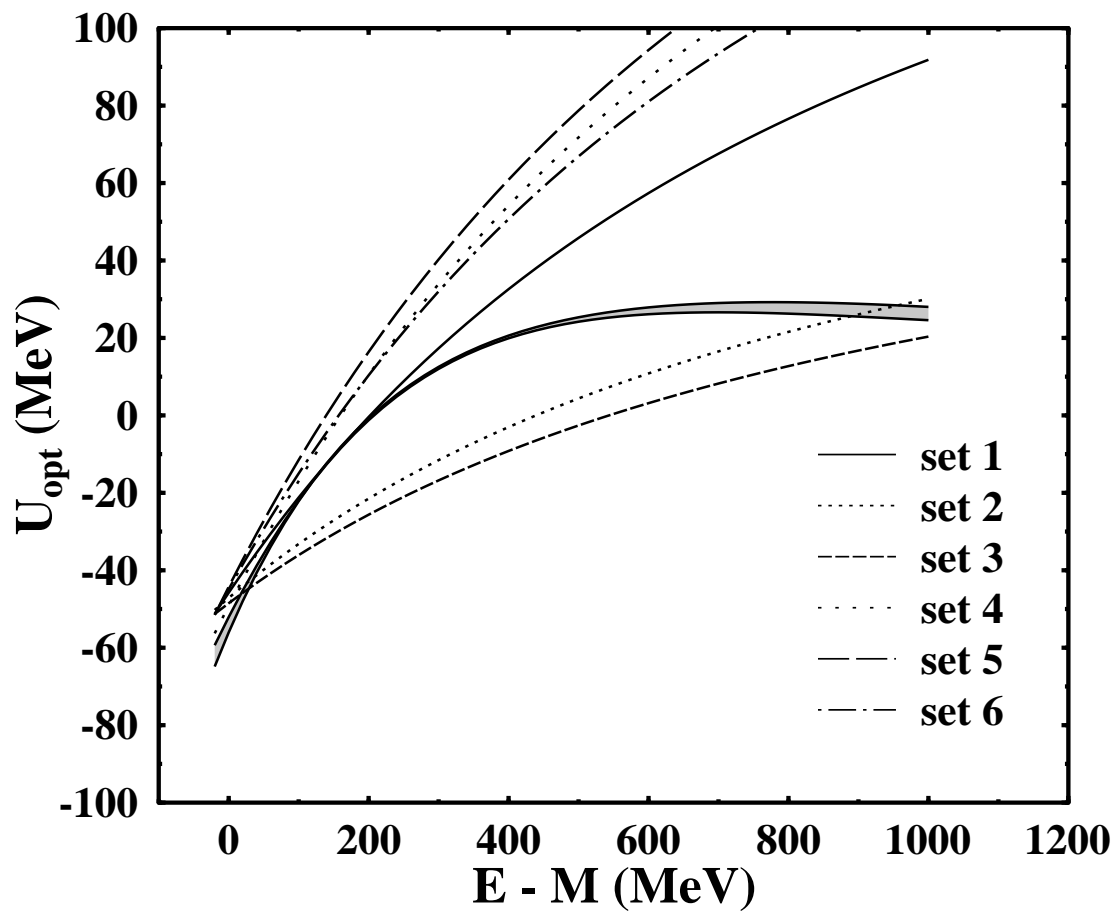


Fig. 3

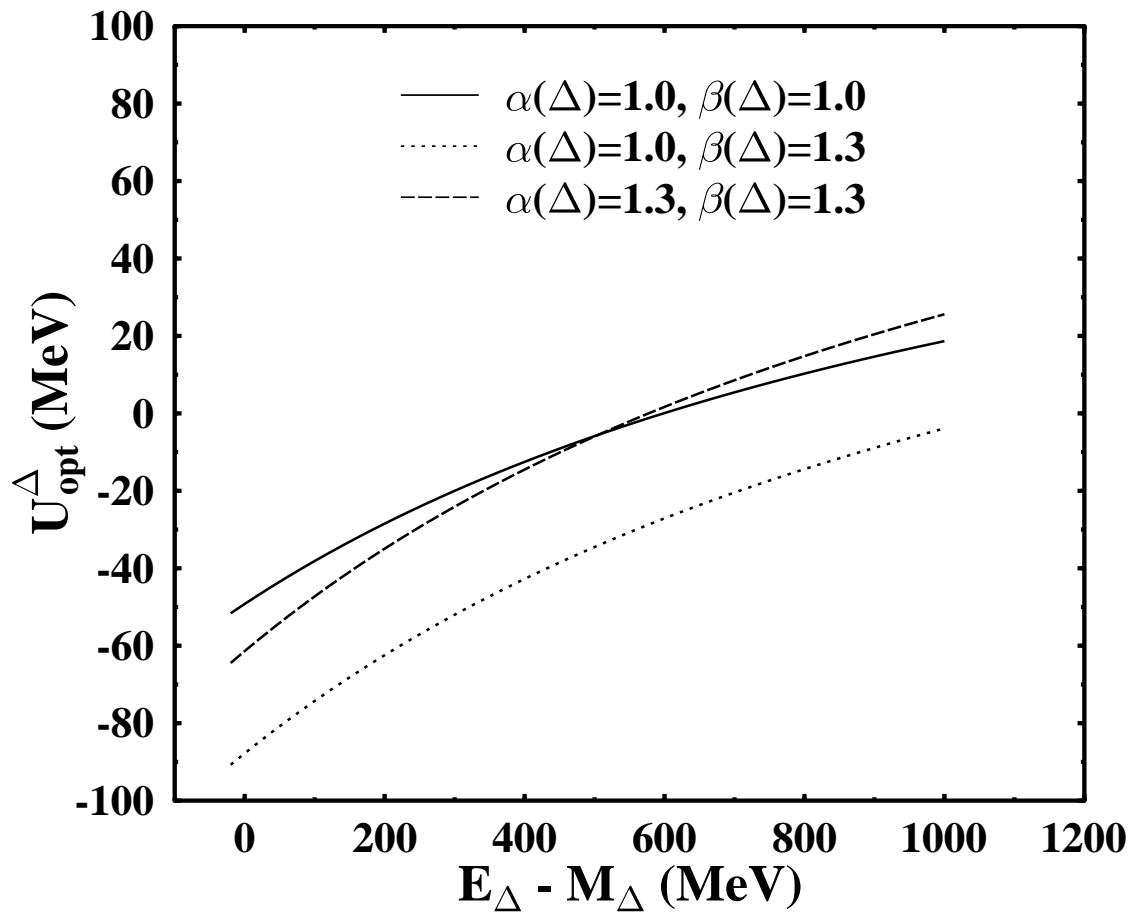


Fig. 4

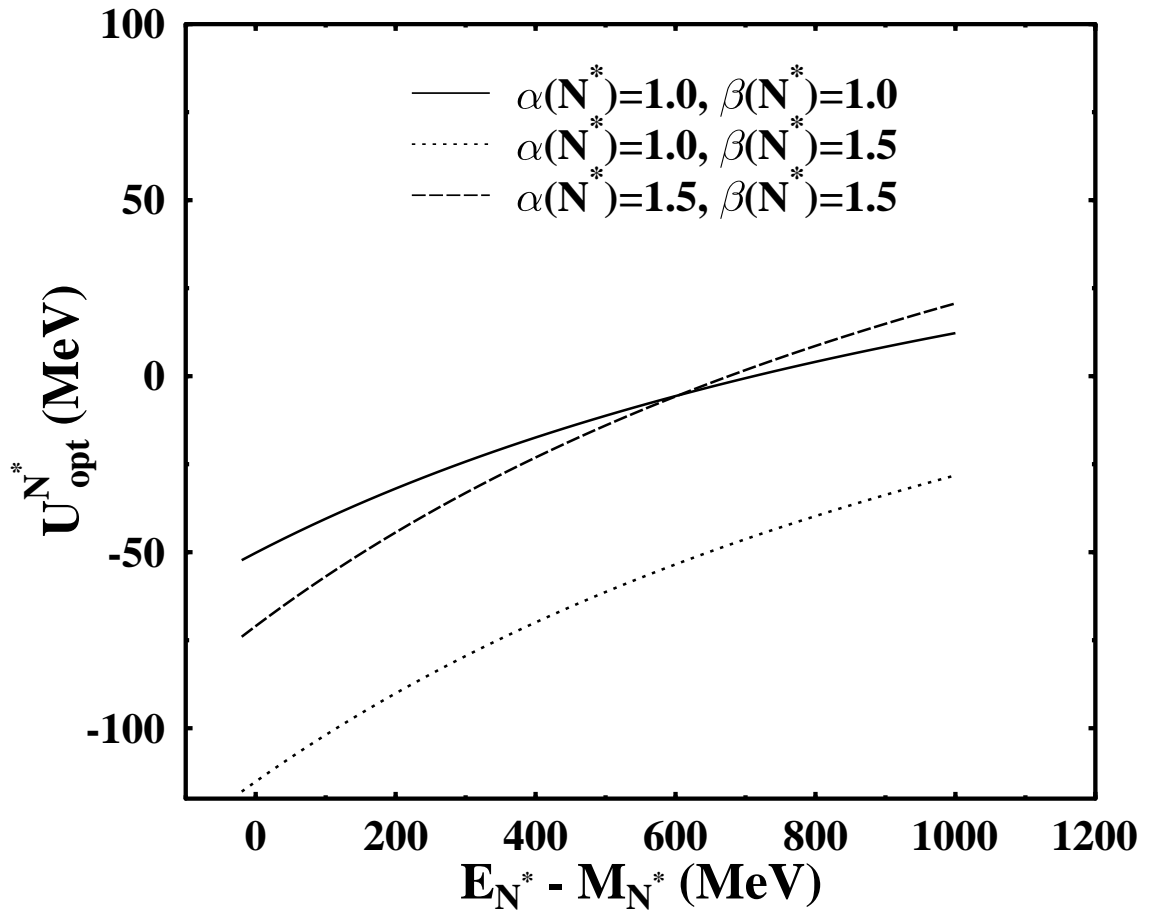


Fig. 5

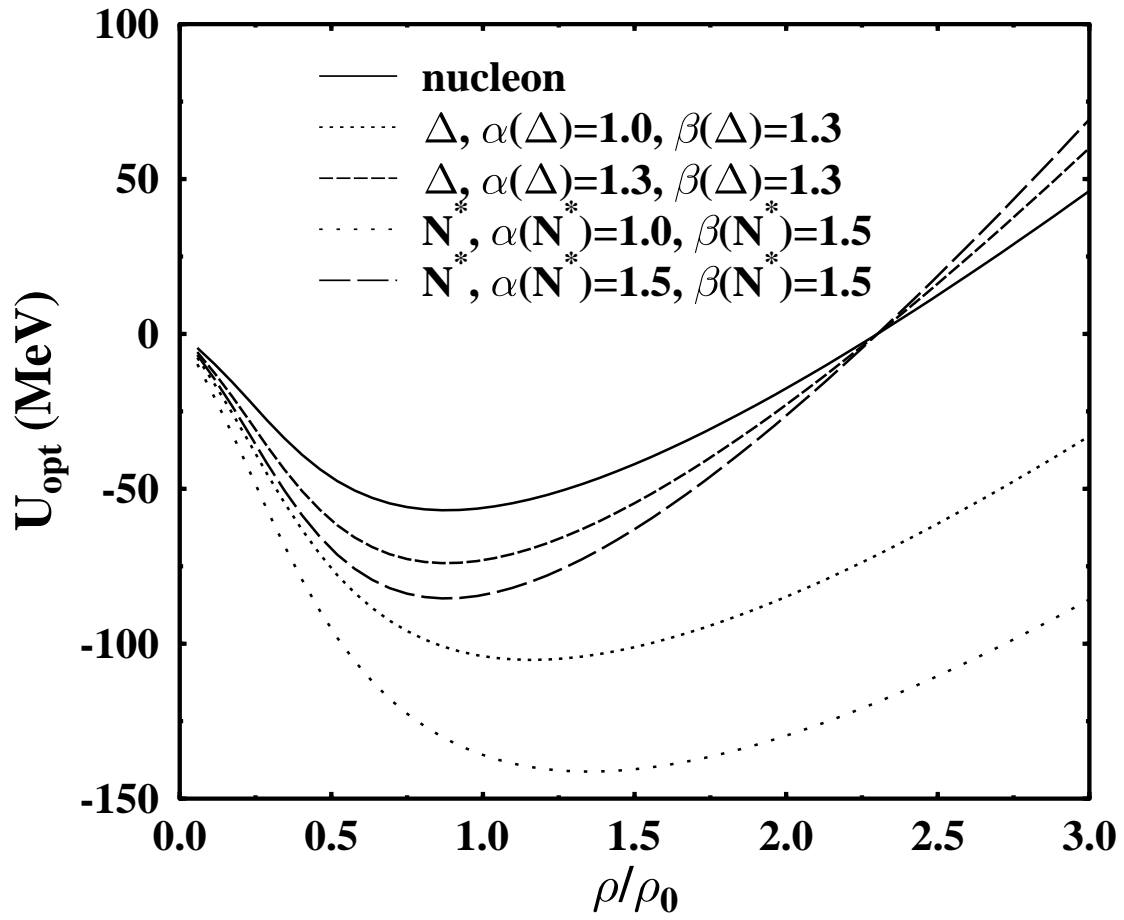




Fig. 6

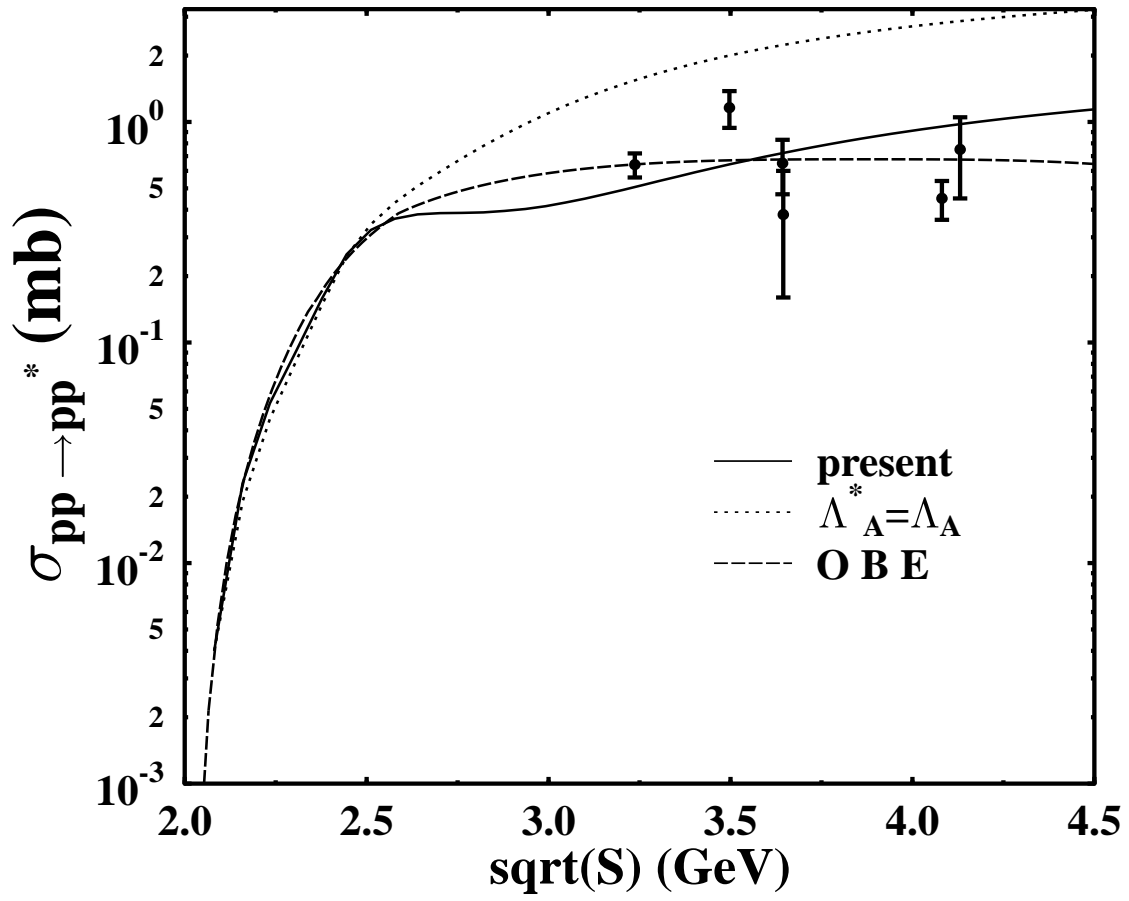


Fig. 7

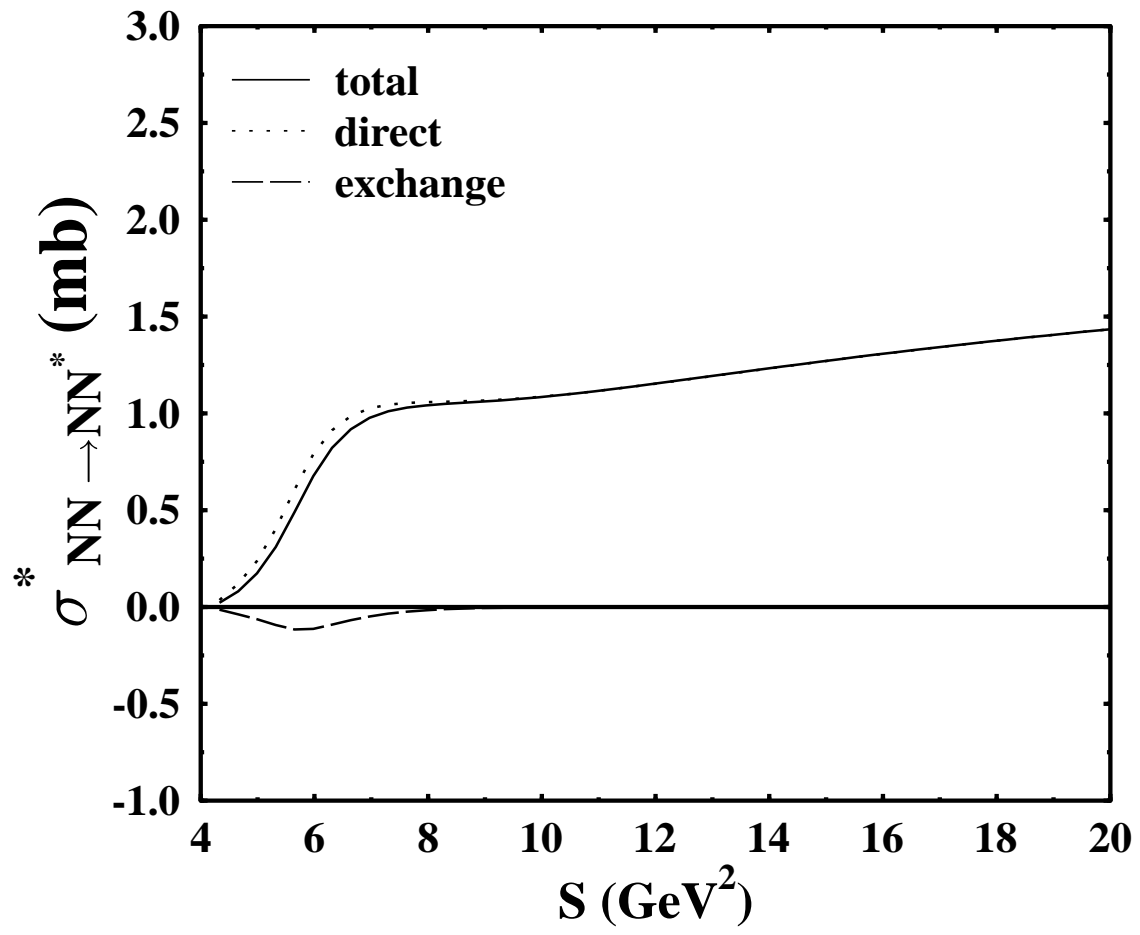


Fig. 8

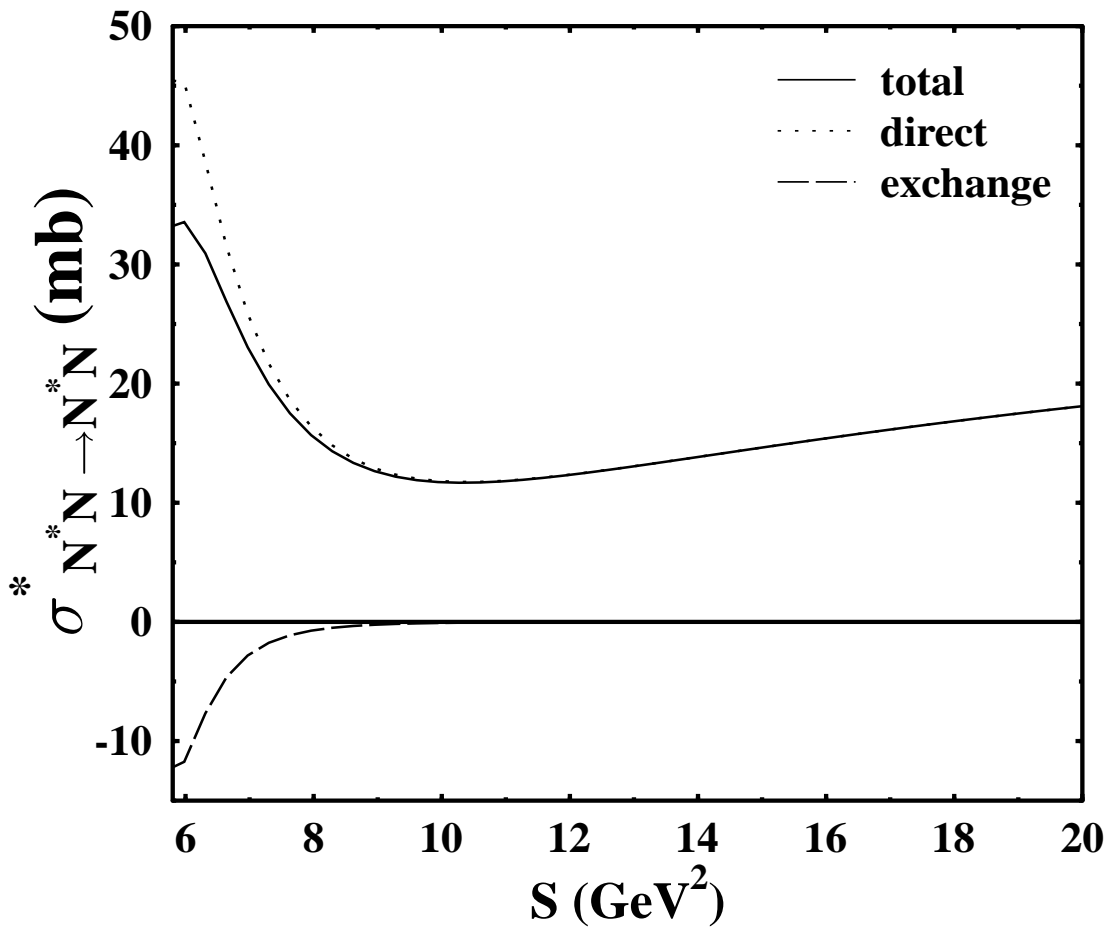


Fig. 9

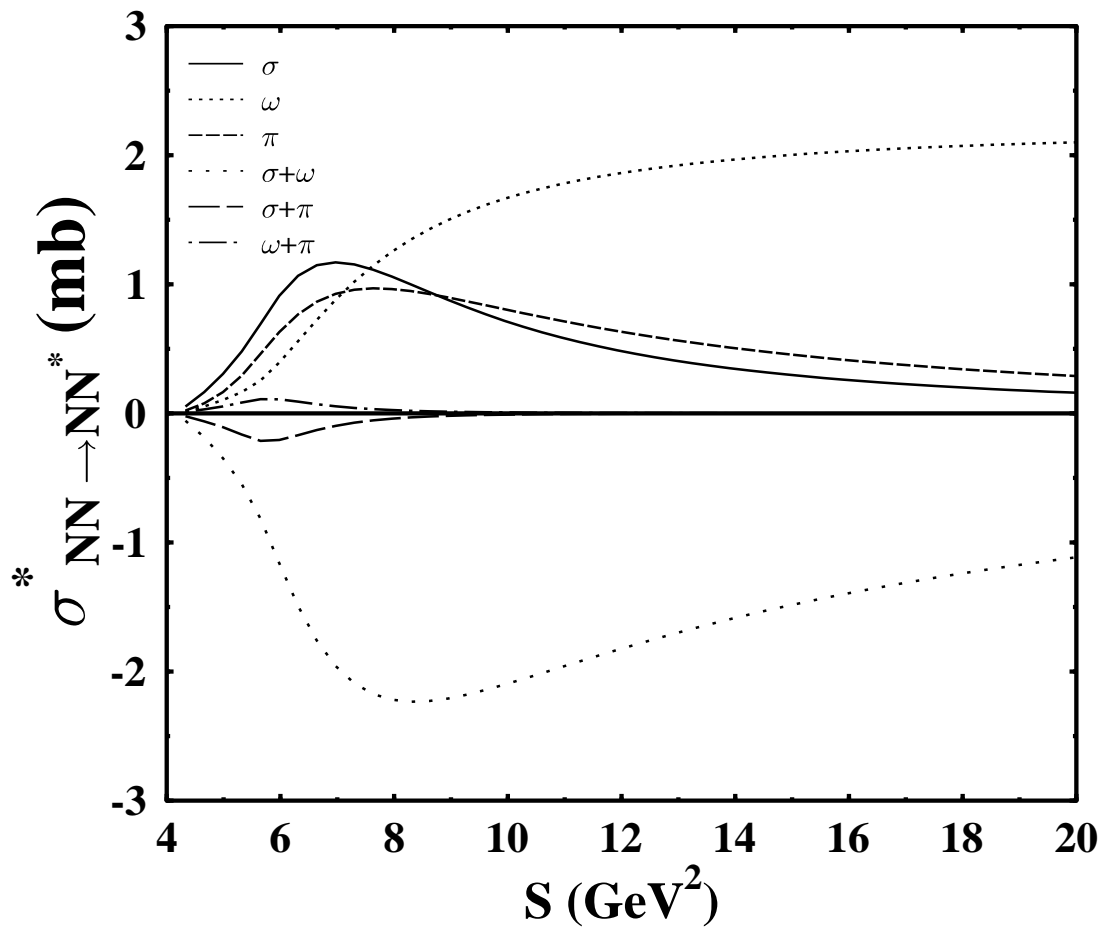


Fig. 10

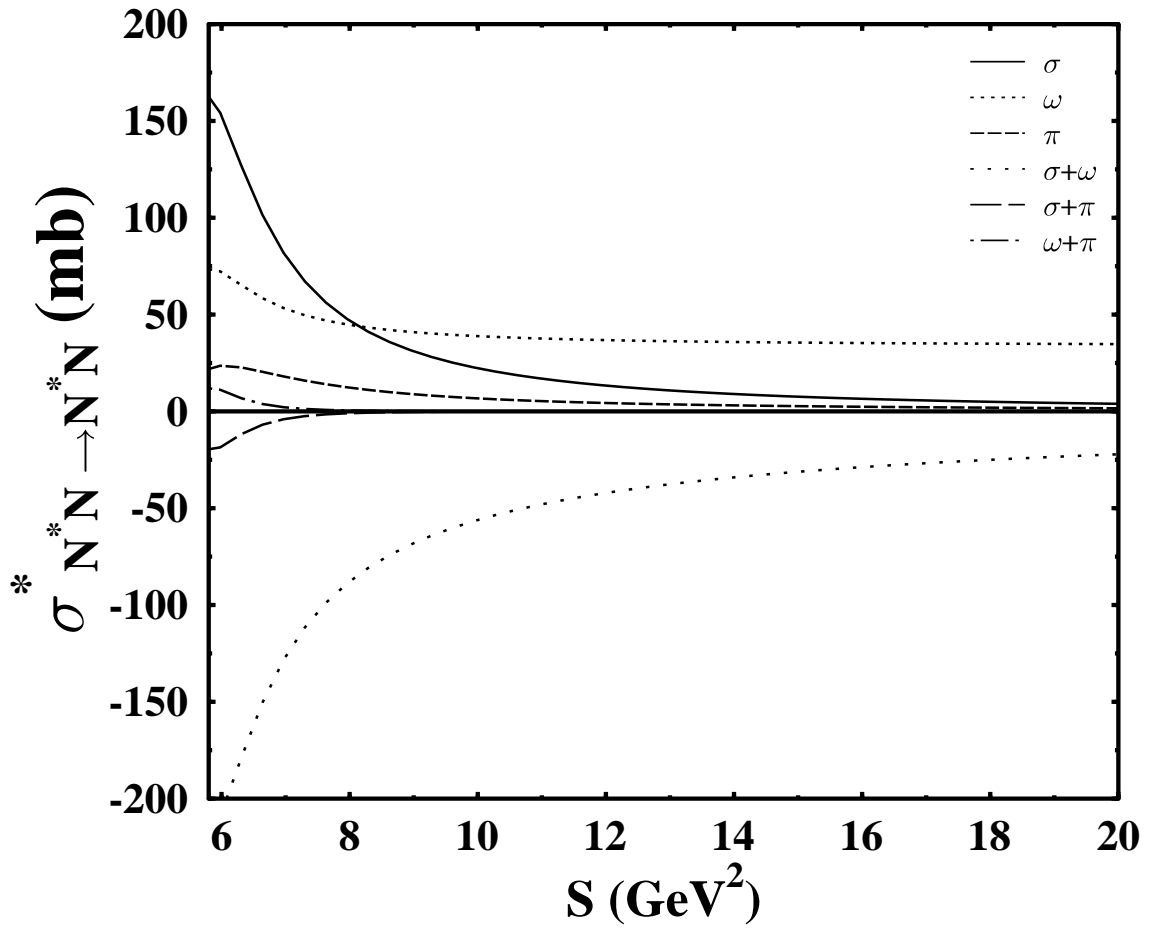


Fig. 11

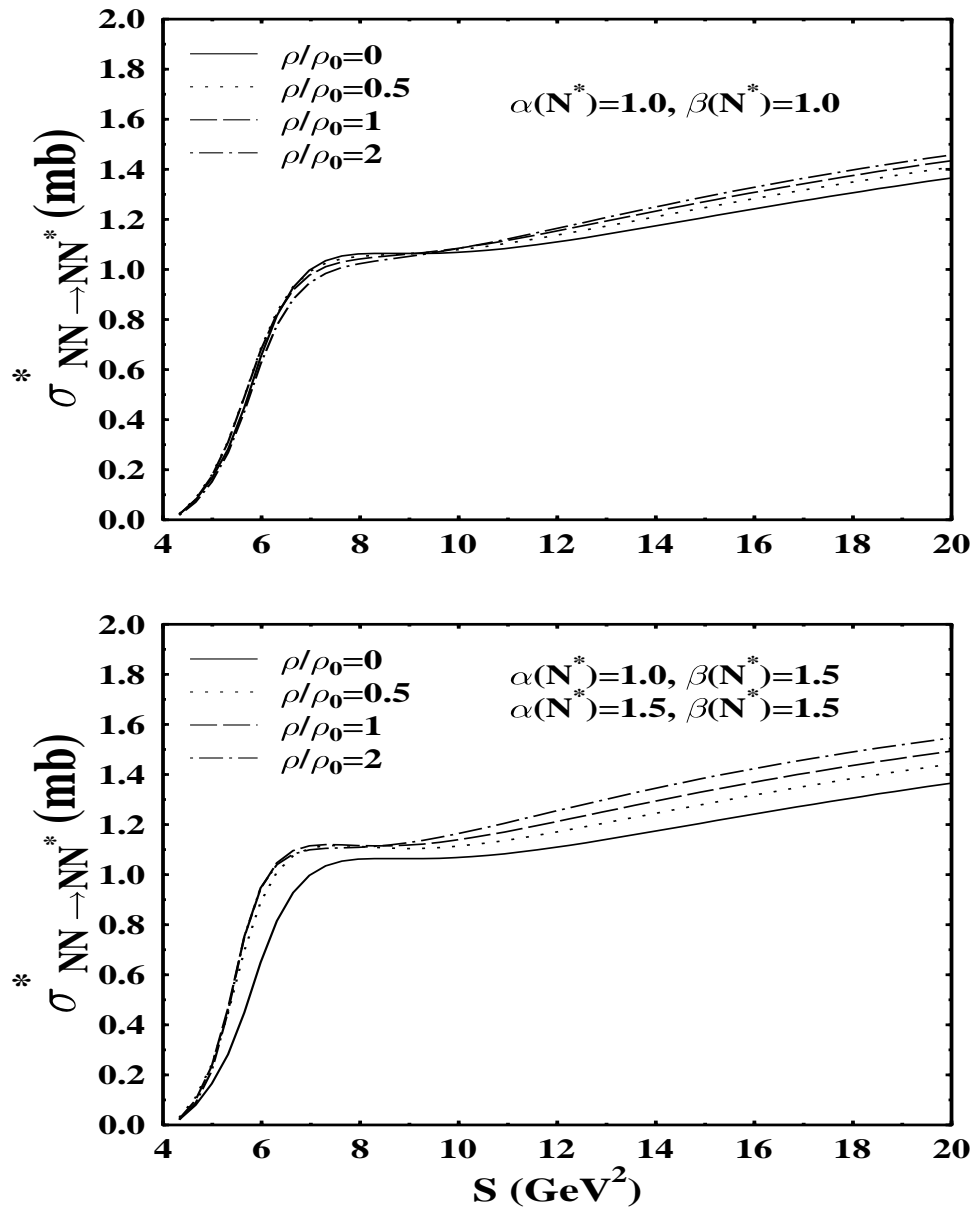


Fig. 12

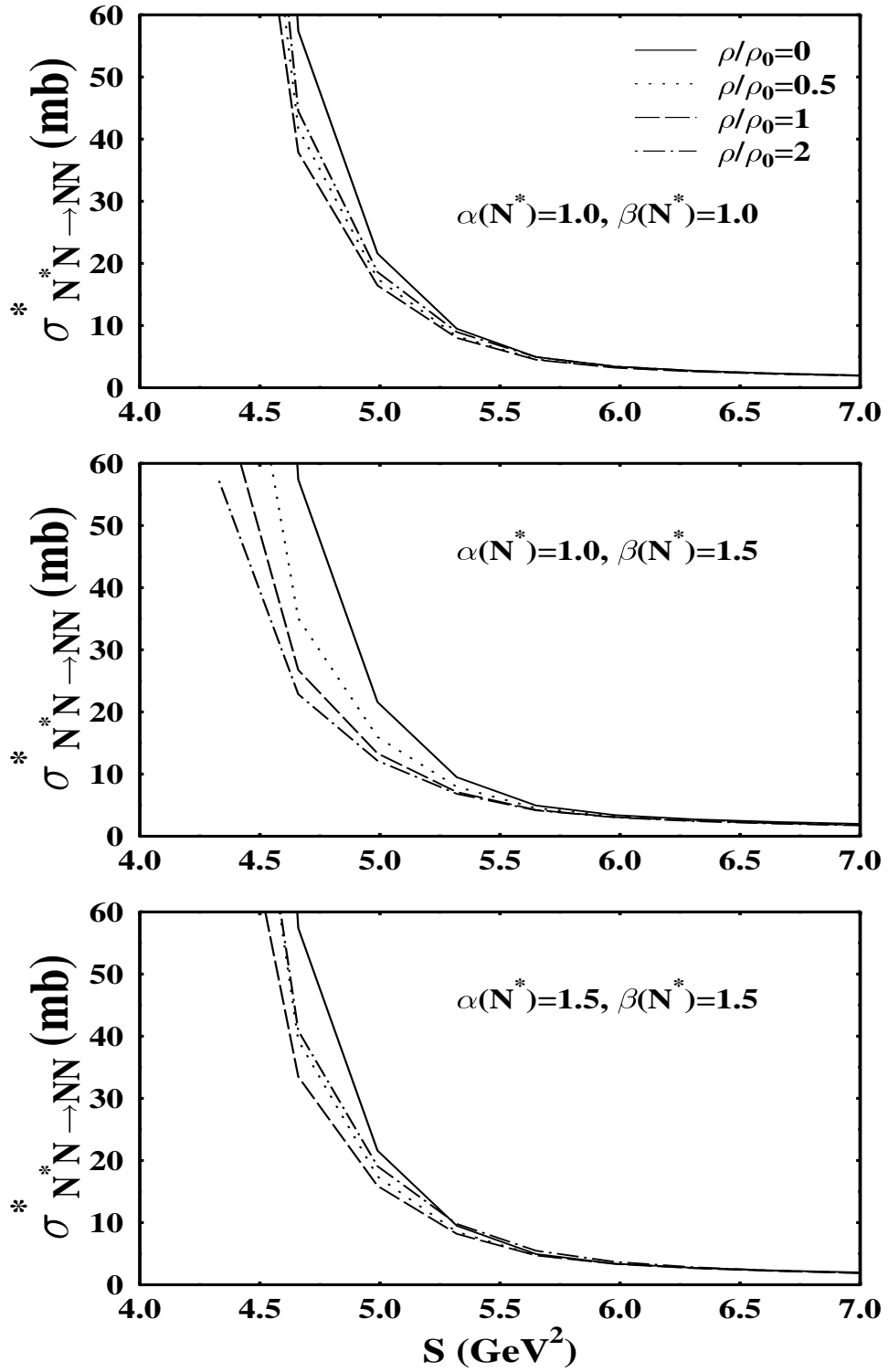


Fig. 13

